Mathematical Modeling of Dengue Viral Infection

Ryan P. Nikin-Beers

Thesis submitted to the Faculty of the
Virginia Polytechnic Institute and State University
in partial fulfillment of the requirements for the degree of

Master of Science
in
Mathematics

Stanca M. Ciupe, Chair
Matthias Chung
Yuriko Y. Renardy

May 5, 2014
Blacksburg, Virginia

Keywords: Dengue Fever, Mathematical Modeling, Antibody-Dependent Enhancement

Mathematical Modeling of Dengue Viral Infection

Ryan P. Nikin-Beers

(ABSTRACT)

In recent years, dengue viral infection has become one of the most widely-spread mosquito-borne diseases in the world, with an estimated 50-100 million cases annually, resulting in 500,000 hospitalizations. Due to the nature of the immune response to each of the four serotypes of dengue virus, secondary infections of dengue put patients at higher risk for more severe infection as opposed to primary infections. The current hypothesis for this phenomenon is antibody-dependent enhancement, where strain-specific antibodies from the primary infection enhance infection by a heterologous serotype. To determine the mechanisms responsible for the increase in disease severity, we develop mathematical models of within-host virus-cell interaction, epidemiological models of virus transmission, and a combination of the within-host and between-host models. The main results of this thesis focus on the within-host model. We model the effects of antibody responses against primary and secondary virus strains. We find that secondary infections lead to a reduction of virus removal. This is slightly different than the current antibody-dependent enhancement hypothesis, which suggests that the rate of virus infectivity is higher during secondary infections due to antibody failure to neutralize the virus. We use the results from the within-host model in an epidemiological multi-scale model. We start by constructing a two-strain SIR model and vary the parameters to account for the effect of antibody-dependent enhancement.

Contents

List of Figures

List of Tables

Chapter 1

Introduction

The outline of the thesis is described as follows. We begin the second chapter by first giving a brief overview of the biology of the immune system, followed by a description of dengue viral infection and its epidemiology. We then describe the current hypothesis for why more cases of dengue hemorrhagic fever have been seen recently, known as antibody-dependent enhancement. We also describe the problems that face those trying to develop a vaccine against dengue. In the third chapter, we give an overview of the mathematics behind different modeling techniques of the biological behaviors described in the second chapter. We split this into three parts: within-host modeling, which describes the interaction between virus and the immune system; epidemiological modeling, which describes the nature of an infection throughout a population; and multi-scale modeling, which combines within-host modeling and epidemiological modeling. In each of these instances, we give an overview of the modeling techniques in general, and then explain work that has been done using these models that is dengue-specific. In the fourth chapter, we formulate a within-host model of dengue viral infection. Due to the nature of the dengue virus, we differentiate between primary and secondary infections. Details are found in chapter two. We thus develop two models to account for these differences. In each case, we prove that with positive initial conditions, the solutions are positive and bounded, as to make sense biologically. We determine the steady states of each model and their stability. We use published data to fit our models and perform a sensitivity analysis for estimated parameters. We finish this section by discussing the implications of our results. In the fifth chapter, we modify an existing epidemiological model of dengue [7] and discuss its behavior. In the sixth chapter, we modify the epidemiological model described in the fifth chapter using the conclusions reached through within-host modeling. We conclude in the seventh chapter with a summary of our future work, which relates mostly to multi-scale modeling of dengue viral infection.

Chapter 2

Biological Background

2.1 The Immune System

The immune system responses are processes in which the host fights off an infection due to a foreign particle, which in our case is a virus. The response consists of two parts: the innate immunity, which is non-specific and contains no memory; and adaptive immunity, which is pathogen-specific and relies on memory of previous infections [1]. We will focus on outlining the adaptive immune response since it relates to dengue viral infection. Adaptive immune responses can be split into two types of responses, one carried out by B-cells (antibody response) and the other carried out by T-cells (cell-mediated immune response) [1]. The antibody response activates B-cells, which mature into plasma cells which then produce antibodies. The antibodies travel through the bloodstream and bind to the infiltrating virus. Antibody functions can be split into two categories: neutralizing and non-neutralizing. When bound to neutralizing antibodies, the virus no longer has the ability to bind to receptors on target cells, thus making the virus unable to infect and therefore neutralizing the virus [1]. Non-neutralizing antibodies only mark the virus, which can still infect, so that phagocytes, cells that exist specifically to ingest anything harmful to the body, can destroy them. In cell-mediated immune responses, activated T-cells eliminate infected cells that have virus proteins on their surface, causing infected cells to be destroyed before the virus is allowed to replicate [1]. A figure of the adaptive immune response is shown below.

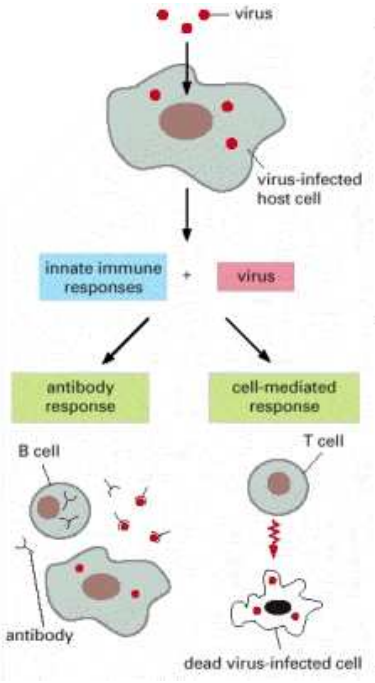

Figure 2.1: The adaptive immune response [1].

2.2 Dengue Viral Infection

Dengue viral infection is a mosquito-borne disease which evolves into either dengue fever (DF), dengue hemorrhagic fever (DHF) or dengue shock syndrome (DSS) depending on certain host factors. DF is largely asymptomatic, where the worst cases result in mild symptoms such as rash, headache, and nausea [11]. However, DHF and DSS are severe illnesses, with DHF typified by high blood platelet count, bleeding, and liver damage, while DSS results in symptoms such as high blood pressure, internal bleeding, and possible shock if not treated in a proper time span [15]. The estimated number of cases a year is in the range of 50-100 million, resulting in 500,000 hospitalizations, making dengue one of the most difficult mosquito-borne diseases in the world [11].

Dengue virus consists of four serotypes, usually labeled DENV 1-4. Once patients become infected with one of the serotypes, strain-specific antibodies are produced and patients develop lifelong immunity against any homologous serotype [15]. This is known as the period of primary infection, and will most often be either asymptomatic or result in mild dengue fever. Patients also undergo a three-month period of cross-protection where they become immune to the other three serotypes [13]. After this period of immunity has elapsed, if they are at some later point infected with a heterologous serotype, they are at increased risk of

developing DHF, and will most likely suffer a more severe form of illness than they experienced during primary infection [15]. One hypothesis for why this occurs is discussed in the next section. Although tertiary and quaternary infections are in theory possible, they are rare. It is assumed that immunity from all four serotypes develops after secondary infection [13].

Illnesses with DF-like symptoms have been described as far back as 400 AD, but the first case of DHF was discovered relatively recently, in approximately 1953 [11]. Since then, there have been many large-scale epidemics of DHF, mostly in tropical regions [15]. The disease is spread through human contact and contact with the species Aedes aegypti [11]. The clearest example of DHF-outbreak has been in the Central and South Americas, after its mosquito-elimination program was discontinued in the 1970s [11]. Specifically in Cuba, DENV-1 was brought into the country in 1977, resulting in approximately half of the population becoming infected, mostly asymptomatic, with some mild cases of dengue fever [15]. However, in 1981, when DENV-2 was introduced into the country, much more severe cases of dengue were seen, including DHF/DSS. Those that had secondary infection were more likely to develop severe disease [15]. It has been hypothesized that the cause of these outbreaks can be attributed to multiple strains of the virus circulating in the same region, leading to increased incidence of cases of DHF.

2.3 Antibody-Dependent Enhancement

The recent epidemics of DHF have been ascribed to a hypothesis known as antibody-dependent enhancement (ADE). As described previously, during dengue primary infection, strain-specific antibodies are produced as an immune system response to the virus [13]. However, after the period of cross-protection, if a host is infected with a heterologous serotype, there is increased risk of severe infection [37]. This is thought to be caused by the antibodies that are produced as a response to the primary infection. Normally, neutralizing antibodies bind to the virus, which then attach to FcγR receptors on a host cell, which trigger either phagocytosis or antibody-dependent cytotoxicity, two processes which allow the virus to be destroyed [41]. These FcγR receptor-bearing cells are not normally infected with virus. However, in antibody-dependent enhancement, since the strain-specific antibodies from the primary infection are present, they bind to the secondary dengue virus and attempt to neutralize it. However, the antibodies from the primary infection are not able to neutralize the secondary dengue virus, thus allowing the FcγR receptor-bearing cells to become infected when they ingest antibody-virus complexes [41]. This leads to more cells becoming infected, which leads to more virus being produced in the body, which leads to more severe infection.

2.4 Original Antigenic Sin

Another hypothesis that may describe the behavior of dengue infection is that of original antigenic sin. In this scenario, the immune response to a secondary infection of a heterologous serotype is dominated by effector cells specific to primary infection. However, these effector cells have a lower affinity for the secondary virus, meaning they are not able to clear the secondary virus as easily [29]. This is different than antibody-dependent enhancement since the effector cells can be activated sooner than the antibody response for a secondary infection.

2.5 Vaccination

Although there is an ongoing dengue vaccine trial being tested [24], there is currently no vaccine to protect against all dengue virus serotypes. The main problem with vaccinating against the dengue virus is that if a population is vaccinated against only one strain, it is as if the population has been subject to a primary infection [41]. The vaccination program thus puts the entire population at risk for more severe infection than they otherwise would have been if the vaccine program had not been implemented. Therefore, it has been suggested that a vaccination program must induce a long-lasting antibody response against all four serotypes simultaneously in order to be effective at preventing severe infection from occurring [41]. Also, problems may arise if not enough people are vaccinated, as those who are asymptomatic due to vaccination will be able to transmit the disease.

Chapter 3

Mathematical Background

3.1 Introduction

Mathematical modeling can be used to simulate a series of processes over time. Specifically in regards to biological models, we can better understand the underlying causes of infection in an individual (within-host modeling) or infection in a population (epidemiological modeling). Models can be used to estimate parameters that we do not have the means of measuring in a laboratory by fitting a model simulation to known data. Models can also predict the future behavior of diseases depending on certain conditions [43]. Most importantly, the models can be used to further guide biological experiments.

3.2 Within-Host Modeling

We can model the dynamics of a virus inside a host using a system of three ordinary differential equations. This model does not factor in an immune response and only considers the interactions between target cells T, infected cells I, and the virus V. Over time, if the target cells and virus interact at rate β, then these target cells become infected. Infected cells die at rate δ and produce more virus at rate p. The virus is cleared at rate c. Thus, the model is

$$\begin{aligned} \frac{dT}{dt} &= -\beta TV \\ \frac{dI}{dt} &= \beta TV - \delta I \\ \frac{dV}{dt} &= pI - cV \end{aligned} \tag{3.1}$$

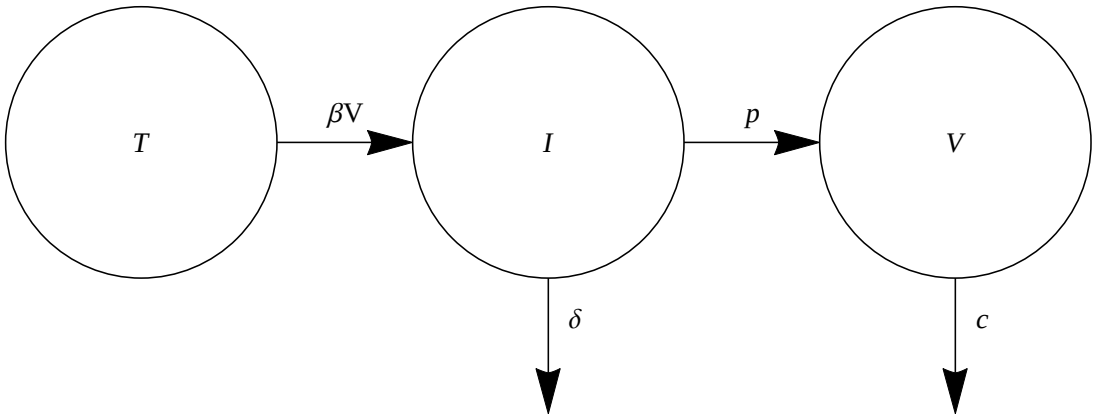

Figure 3.1: The cell-virus interaction in the body.

Variations of this model, some including source and death rates for target cells, have been used to simulate other viral infections such as influenza, HIV, HBV, and HCV [20, 3, 32, 5, 42, 10]. Most other mathematical models of within-host dynamics of a virus will be a variation on the above model, albeit with more equations and more terms depending on what the researcher is studying. Immune responses can be modeled by including terms to represent different immunological factors, such as B-cells, T-cells, and antibodies [6, 35]. Since we have a system of differential equations, we can then study the model to find the steady states, whether they are stable or unstable, and determine what conditions must be satisfied in order to achieve these results. There may be some steady states that have no biological significance, and can thus be ignored. Also, when modeling biological systems, it is important to have a model such that all of the terms are positive and bounded so the system is biologically reasonable.

There have been few attempts to model the within-host dynamics of DENV [34], as most mathematical models of DENV have focused on its epidemiology. We formulate a model which describes the within-host dynamics of primary and secondary DENV in chapter four.

3.3 Epidemiological Modeling

We can model the epidemiology of a virus in a population in a similar fashion to how we model the within-host dynamics. The simplest model is a system of three ordinary differential equations showing the interaction between those that are susceptible to the virus S, those that are infected with the virus I, and those that are recovered from the infection R [21]. We assume that the susceptible and the infected interact at rate β, and that the infected

recover at rate v. Thus, the model is

$$\begin{aligned} \frac{dS}{dt} &= -\beta SI \\ \frac{dI}{dt} &= \beta SI - vI \\ \frac{dR}{dt} &= vI \end{aligned} \tag{3.2}$$

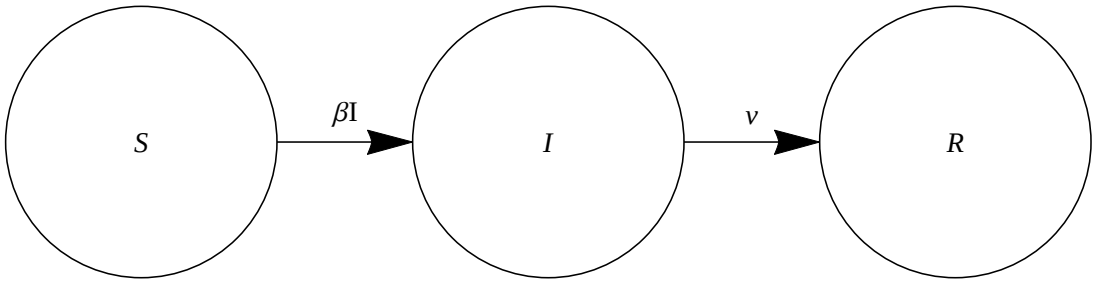

Figure 3.2: The SIR model.

Again, as this is the simplest model possible for describing the population dynamics as a virus works its way through a population, terms and parameters can be added based on the specific dynamics of the virus. We can again analyze the steady states and determine their stability, making sure that all the terms are positive and bounded, so as to be biologically reasonable. Often the model will use proportions so that $S + I + R = 1$. This allows for more complex models to be simplified since one variable can be written in terms of the two others.

As opposed to the within-host model, much work has been done on modeling the dynamics of the epidemiology of the dengue virus. We review two approaches that have been taken recently.

We describe a model which considers two serotypes circulating in the same area, and distinguishes between those with primary infection and those with secondary infection [7]. The transmission rate of those with secondary infection is assumed to be different from those with primary infection by a rate of enhancement. Using overlapping compartments, we define s as those who have been infected with neither serotype, x_i as those who have been infected with serotype i, y_i as those who are currently infected with serotype i, and y_{ij} as those who are currently infected with serotype j having been previously infected with serotype i. Note that x_i contains y_i and y_{ji}. Therefore, at any one time, a member of the population is either in s, in solely one of the x_i, or in both of the x_i. We define the force of infection λ_i as

$$\lambda_i = \beta(y_i + \phi_i y_{ji}) \tag{3.3}$$

This takes into account the transmission probability of the virus β_i and the enhancement effect $\phi_i > 1$ of having a secondary infection. The birth/death rate μ and the length of infection $\frac{1}{\sigma}$ are also taken into account.

The model structure is as follows.

$$\begin{aligned}
\frac{ds}{dt} &= \mu - s\lambda_1 - s\lambda_2 - \mu s \\
\frac{dy_1}{dt} &= s\lambda_1 - \sigma y_1 \\
\frac{dy_2}{dt} &= s\lambda_2 - \sigma y_2 \\
\frac{dy_{12}}{dt} &= (1 - x_2 - s)\lambda_2 - \sigma y_{12} \\
\frac{dy_{21}}{dt} &= (1 - x_1 - s)\lambda_1 - \sigma y_{21} \\
\frac{dx_1}{dt} &= (1 - x_1)\lambda_1 - \mu x_1 \\
\frac{dx_2}{dt} &= (1 - x_2)\lambda_2 - \mu x_2
\end{aligned} \tag{3.4}$$

The model results in oscillatory behavior which is consistent with what has been observed in outbreaks of dengue epidemics.

We modify this model in chapter 5 in order to make it easier to work with by dividing the overlapping compartments into non-overlapping compartments.

We now discuss a more complicated model including a latent stage E_i, cross-protection C_i, and a vector population V_i [40]. The forces of latency ϵ_{V_i} and infection λ_{V_i} exerted by the vector and the forces of latency ϵ_{H_i} and infection λ_{H_i} exerted by hosts are also included. The

model structure is as follows

$$
\begin{aligned}
\frac{dS_0}{dt} &= (N_H - S_0)\mu_H - (\lambda_{V_1} + \lambda_{V_2})\frac{S_0}{N_H} \\
\frac{dE_i}{dt} &= \lambda_{V_i}\frac{S_0}{N_H} - \phi_j\lambda_{V_j}\frac{E_i}{N_H} - (\sigma_H + \mu_H)E_i \\
\frac{dI_i}{dt} &= \sigma_H E_i - \phi_j\lambda_{V_j}\frac{I_i}{N_H} - (\gamma_i + \mu_H)I_i \\
\frac{dC_i}{dt} &= \gamma_i I_i - \epsilon_j\lambda_{V_j}\frac{C_i}{N_H} - (\delta_i + \mu_H)C_i \\
\frac{dS_i}{dt} &= (1-p_i)\delta_i C_i - \chi_j\lambda_{V_j}\frac{S_i}{N_H} - \mu_H S_i \\
\frac{d\epsilon_{H_i}}{dt} &= \lambda_{V_i}\frac{S_0}{N_H} + \eta_i\left(\phi_i\lambda_{V_i}\frac{E_j + I_j}{N_H} + \epsilon_i\lambda_{V_i}\frac{C_j}{N_H} + \chi_i\lambda_{V_i}\frac{S_j}{N_H}\right) - (\sigma_H + \mu_H)\epsilon_{H_i} \\
\frac{d\lambda_{H_i}}{dt} &= \beta_i\sigma_H\epsilon_{H_i} - (\gamma_i + \mu_H)\lambda_{H_i} \\
\frac{dS_{12}}{dt} &= \sum_{i=1}^{2}(1-p_i)(1-p_x)\left(\phi_i\lambda_{V_i}\frac{E_j + I_j}{N_H} + \epsilon_i\lambda_{V_i}\frac{C_j}{N_H} + \chi_i\lambda_{V_i}\frac{S_j}{N_H}\right) - \mu_H S_{12} \\
\frac{dV_{S_i}}{dt} &= (kN_H(1 - a\cos(2\pi t)) - V_{S_i})\mu_V - \lambda_{H_j}\frac{V_{S_i}}{N_H} \\
\frac{d\epsilon_{V_i}}{dt} &= \lambda_{H_i}\frac{V_{S_i}}{N_H} - (\sigma_V + \mu_V)\epsilon_{V_i} \\
\frac{d\lambda_{V_i}}{dt} &= \alpha_i\sigma_V\epsilon_{V_i} - \mu_V\lambda_{V_i}
\end{aligned}
\tag{3.5}
$$

This model also leads to oscillations consistent with dengue data if cross-immunity and strong ADE effects are observed. Interestingly, we can derive the first model from the second model by setting

$$\lambda_{V_i} = \frac{\alpha_i k\sigma_V\lambda_{H_i}}{\mu_V(\sigma_V + \mu_V)} \tag{3.6}$$

and $V_{S_i} = kN_H$ and $\frac{1}{\sigma_H} \to 0$, $\phi_i = \epsilon_i = \chi_i = 1, \eta_i > 1$.

3.4 Multi-Scale Modeling

In multi-scale modeling, we relate within-host and epidemiological models. We review two examples of multi-scale models that differ in their approach.

One multi-scale model studying the effects of temperature on influenza fitness [18] first begins with a simple within-host model similar to 3.1 to describe the within-host dynamics of the influenza virus. The epidemiological model is similar to 3.2, but includes a term for the

virus that exists in the environment. So using constant rates for the rate of transmission b_1 between infected hosts I and susceptible hosts S, the rate of transmission b_2 between pathogen P and susceptible hosts, the recovery rate g of infected hosts, the rate of expulsion w of the virus into the environment by infected hosts, and the natural clearance rate c_b of the virus in the environment, the epidemiological model can be written as

$$\begin{aligned} \frac{dS}{dt} &= -b_1 SI - b_2 SP \\ \frac{dI}{dt} &= b_1 SI + b_2 SP - gI \\ \frac{dP}{dt} &= wI - c_b P \end{aligned} \tag{3.7}$$

The multi-scale model, however, requires that the rate of transmission b_1 between hosts, the rate of expulsion of virus w into the environment by an infected host, and the rate of recovery g of an infected host all depend on the time since the initial infection. So, the multi-scale model can be written as

$$\begin{aligned} \frac{dS(t)}{dt} &= -b_2 S(t)P(t) - S(t)\int_0^\infty b_1(a)I(t,a)da \\ I(t,0) &= b_2 S(t)P(t) + S(t)\int_0^\infty b_1(a)I(t,a)da \\ \frac{\partial I(t,a)}{\partial t} &= -\frac{\partial I(t,a)}{\partial a} - g(a)I(t,a) \\ \frac{dP(t)}{dt} &= \int_0^\infty w(a)I(t,a)da - c_b P(t) \end{aligned} \tag{3.8}$$

The model is shown in Fig 3.3.

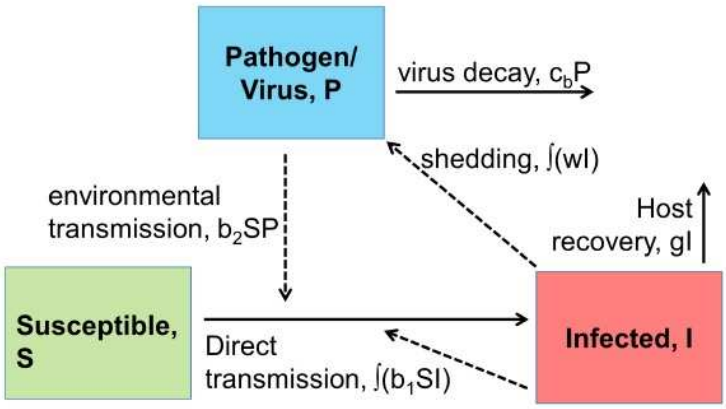

Figure 3.3: A diagram of the multi-scale model described in Chapter 3.4 [18].

This requirement combines the two models because $b_1(a)$ and $w(a)$ depend on the amount of virus within an infected host. To make the model simpler, they assume that all infected hosts are infectious for a fixed period D. However, this depends on the within-host model as well, since D can be determined from the length of time the graph of the virus in the within-host model stays above a certain threshold. In this case $g(a)$ is a Dirac-delta function. The multi-scale model is mainly used to determine $R_0 = R_d + R_e$, where R_0 is the basic reproductive number, which estimates the number of new infections caused by an infected host; R_d is the number of new infections caused by direct contact; and R_e is the number of new infections caused by the environment after virus is expelled from the infected host. Since $b_1(a)$ and $w(a)$ both depend on the viral load, they determine that

$$\begin{aligned} R_d &= S(0)h_1 \int_0^D f(V(a))da \\ R_e &= \frac{b_2 h_2 S(0)}{c_b} \int_0^D f(V(a))da \end{aligned} \tag{3.9}$$

where $f(x)$ is a real valued function. They look at three different functions

$$\begin{aligned} f_1(x) &= x \\ f_2(x) &= \frac{5x\log(x)^5}{2.5^5 + \log(x)^5} \\ f_3(x) &= \log(x) \end{aligned} \tag{3.10}$$

They then have data which relates the rate of decay of a strain of influenza virus to the temperature. Based on this data, they determine c_w, the within-host viral clearance rate, and c_b, the multi-scale model viral clearance rate, since they assume temperature in the body is 40 degrees Celsius and temperature in the environment is 5 degrees Celsius. The other parameters of the within-host model were determined from previous studies. Thus, from running the within-host model, they determine the viral load over time, which allows them to calculate the fitness of R_d and R_e for influenza strains relative to a reference strain, where the constants of R_d and R_e cancel out.

By analyzing the results of these models, they find that if R_d and R_e use f_3, there is evolutionary pressure for strains of influenza to persist at high temperatures. If f_1 or f_2 are used for R_d and R_e, then influenza strains that persist at low temperatures have highest fitness. The results show that the fitness of influenza strains depends on the viral load within a host, which can only be obtained by studying the multi-scale model.

Instead of partial differential equations, the multi-scale model described by Heffernan [19] adds compartments to an epidemiological model based on the results of a within-host model.

They first develop a within-host model for measles which includes memory CD8 T-cells. Based on this model, they then add compartments to the basic SEIR model (like the SIR

model but including a compartment for exposed but not infected) which correspond to individuals who have different levels of memory CD8 T-cells, some due to natural infections and those due to vaccination. These compartments are separated since vaccination results in lower memory cell levels as compared to those who have been exposed to natural infection. The equations are

$$\begin{aligned}
\frac{dS_0}{dt} &= B(1-p) + qR_0 + w_1 S_1 - \lambda S_0 - dS_0 \\
\frac{dS_v}{dt} &= Bp + qR_v + w_{v+1} S_{v+1} - \lambda S_v - dS_v - w_v S_v \\
\frac{dS_i}{dt} &= qR_i + w_{i+1} S_{i+1} - \lambda S_i - dS_i - w_i S_i \forall i \neq 0, v \\
\frac{dE_i}{dt} &= \lambda S_i - a_i E_i - dE_i \\
\frac{dI_i}{dt} &= a_i E_i - g_i I_i - dI_i \\
\frac{dR_i}{dt} &= w_{i+1} R_{i+1} + \sum_j b_{ij} g_j I_j - w_i R_i - qR_i \\
\lambda &= \sum_i \beta_i I_i
\end{aligned} \tag{3.11}$$

S_i and R_i now refer to those who will get a boosting effect in their memory levels from infection and those who will not, respectively. The number v is fixed such that vaccination immediately gives an individual some form of immune memory, albeit not as high as if an individual had actually been infected. In this case, they use the parameters $v = 90$, while $i = 0, 1, ..., 178$. The parameters for the rate of exposure a_i, the rate of infection g_i, the transmission rate β_i, and the boosting effect b_{ij} from memory level i to memory level j due to infection are determined by the within-host model, which makes this a multi-scale model. The w_i represents the rate of waning immunity over time, q represents the proportion of those that do see a boost in their immune levels after consecutive epidemics, and B and d are birth and death rates.

They find that, as might be expected, very high levels of vaccination result in eradication of the virus. However, for relatively high levels of vaccination (80%) and moderate waning immunity effects, large cycles are produced. Therefore, by incorporating the results from the within-host model into the epidemiological model, effects can be observed that would not otherwise be able to be studied from the epidemiological model or within-host model alone.

Since multi-scale modeling has only been introduced within the past decade [19], no research has currently been done on multi-scale modeling relating to dengue. In future studies, we plan to incorporate the results from the models described in this paper to develop a sophisticated multi-scale model of dengue viral infection.

Chapter 4

A Within-Host Model of Dengue Viral Infection

4.1 Primary Infection

We model the host-virus dynamics during primary infection with a dengue virus. The model describes the interaction between uninfected monocytes, T, infected monocytes, I, dengue virus, V, resting and activated B lymphocytes, B and B_a, plasma cells, P, and antibody, A, as follows. Uninfected monocytes are produced at constant rate s, die at per capita rate d_T, and become infected at constant rate β. Infected monocytes die at per capita rate $\delta > d_T$ due to both virus-induced and immune-system-induced toxicity [26, 28]. Virus is produced at constant rate p and is cleared at per capita rate c. Naive B-lymphocytes which encounter antigen become activated at constant rate α. Resting and activated B-cells die at per capita rates d_B and d_{B_a}, respectively. A constant fraction k of activated cells become plasma cells in an antigen dependent manner. Plasma cells are maintained in the body for a long time to account for immunological memory. We model this through a logistic term with maximum growth rate r and carrying capacity K_P. They produce antibodies at constant rate N. Antibodies are cleared at per capita rate d_A, reduce viral infectivity at constant rate η, and enhance viral clearance at rate γ. Note that η is the effect on the virus from neutralizing antibodies, whereas γ is the effect on the virus from non-neutralizing antibodies.

The system describing these interactions is given by

$$\begin{aligned}
\frac{dT}{dt} &= s - d_T T - \frac{\beta T V}{1+\eta A}, \\
\frac{dI}{dt} &= \frac{\beta T V}{1+\eta A} - \delta I, \\
\frac{dV}{dt} &= pI - cV - \gamma V A, \\
\frac{dB}{dt} &= -\alpha B V - d_B B, \\
\frac{dB_a}{dt} &= \alpha B V - k B_a V - d_{B_a} B_a, \\
\frac{dP}{dt} &= rP\left(1 - \frac{P}{K_P}\right) + k B_a V, \\
\frac{dA}{dt} &= NP - d_A A.
\end{aligned} \tag{4.1}$$

4.1.1 Analytical Results

In this section we establish the positivity and boundness of the solutions of model (4.1). We assume that the initial conditions for the system have the form

$$\begin{aligned}
&T(0) = T_0 > 0, I(0) = I_0 > 0, V(0) = V_0 > 0, \\
&B(0) = B_0 > 0, B_a(0) = B_{a0} > 0, P(0) = P_0 > 0, A(0) = A_0 > 0.
\end{aligned} \tag{4.2}$$

Proposition 1. *The solutions of system* (4.1) *subject to initial conditions* (4.2) *are positive on* $[0, b)$ *for some* $b > 0$.

Proof. Note that (4.1) is locally Lipschitz at $t = 0$. Therefore, the solution of (4.1) subject to (4.2) exists and is unique on $[0, b)$ for some $b > 0$.

Assume that there exists $t_1 \in (0, b)$ such that $I(t_1) = 0$ and all variables are positive in $(0, t_1)$. For all $t \in [0, t_1]$

$$\frac{dI}{dt} = \frac{\beta T V}{1+\eta A} - \delta I \geq -\delta I. \tag{4.3}$$

Hence, $I(t_1) \geq I_0 e^{-\delta t_1} > 0$, a contradiction. Using similar arguments we can show that $P(t) > 0$ and $A(t) > 0$ for all $b > t \geq 0$.

Assume that there exists $t_1 \in (0, b)$ such that $V(t_1) = 0$ and all variables are positive in $(0, t_1)$. Note that since $A(t) > 0$ for all $b > t \geq 0$, $\gamma A > 0$. Since $A(t)$ is continuous, $A(t)$ is bounded on $[0, t_1]$. So there exists an M_1 such that $M_1 \geq \gamma A > 0$ and

$$\frac{dV}{dt} = pI - cV - \gamma V A \geq -cV - M_1 V = -(c + M_1)V, \tag{4.4}$$

for all $t \in [0, t_1]$. Therefore, $V(t) \geq V_0 e^{-(c+M_1)t} > 0$ for $t \in [0, t_1]$. In particular, $V(t_1) > 0$, which is in contradiction with the $V(t_1) = 0$ assumption.

Assume that there exists $t_1 \in (0, b)$ such that $T(t_1) = 0$ and all variables are positive in $(0, t_1)$. Note that since $A(t) > 0$ and $V(t) > 0$ for all $b > t \geq 0$, $\frac{\beta V}{1+\eta A} > 0$. Since $V(t)$ and $A(t)$ are continuous, they are bounded on $[0, t_1]$. Therefore, there exists an M_2 such that $M_2 \geq \frac{\beta V}{1+\eta A} > 0$ and

$$\frac{dT}{dt} = s - d_T T - \frac{\beta T V}{1 + \eta A} \geq -d_T T - M_2 T = -(d_T + M_2)T, \tag{4.5}$$

for all $t \in [0, t_1]$. This implies that $T(t) \geq T_0 e^{-(d_T+M_2)t} > 0$ for $t \in [0, t_1]$. In particular, $T(t_1) > 0$, which is in contradiction with the $T(t_1) = 0$ assumption.

Assume that there exists $t_1 \in (0, b)$ such that $B(t_1) = 0$ and all variables are positive in $(0, t_1)$. Note that since $V(t) > 0$ and bounded on $[0, t_1]$, there exists an M_3 such that $M_3 \geq \alpha V > 0$ and

$$\frac{dB}{dt} = -\alpha B V - d_B B \geq -M_3 B - d_B B = -(M_3 + d_B)B, \tag{4.6}$$

for all $t \in [0, t_1]$. This implies that $B(t) \geq B_0 e^{-(M_3+d_B)t} > 0$ for $t \in [0, t_1]$. In particular, $B(t_1) > 0$, which is in contradiction with the $B(t_1) = 0$ assumption.

Assume that there exists $t_1 \in (0, b)$ such that $B_a(t_1) = 0$ and all variables are positive in $(0, t_1)$. Note that since $V(t) > 0$ and and bounded on $[0, t_1]$, there exists an M_4 such that $M_4 \geq kV > 0$ and

$$\frac{dB_a}{dt} = \alpha B V - k B_a V - d_{B_a} B_a \geq -k B_a V - d_{B_a} B_a \geq -M_4 B_a - d_{B_a} B_a = -(M_4 + d_{B_a})B_a \tag{4.7}$$

for all $t \in [0, t_1]$. This implies that, $B_a(t) \geq B_{a0} e^{-(M_4+d_{B_a})t} > 0$ for $t \in [0, t_1]$. In particular, $B_a(t_1) > 0$, which is in contradiction with the $B_a(t_1) = 0$ assumption.

Therefore, the system (4.1) subject to the initial conditions (4.2) has positive solutions for all $b > t \geq 0$. □

Proposition 2. *The solution of system* (4.1) *subject to initial conditions* (4.2) *remains bounded on* $[0, b)$ *for some* $b > 0$.

Proof. From Proposition 1 we know that all variables are positive for $b > t \geq 0$. Let $F_1(t) = T(t) + I(t)$ and $m = \min(d_T, \delta)$. Therefore,

$$\frac{dF_1}{dt} = s - d_T T - \delta I \leq s - m(T + I) = s - m F_1, \tag{4.8}$$

which implies that

$$F_1(t) \leq \max\{F_1(0), \frac{s}{m}\}. \tag{4.9}$$

for $t \in [0, b)$. Since $T(t) > 0$ and $I(t) > 0$, for $t \in [0, b)$ we have that $T(t)$ and $I(t)$ are bounded for $t \in [0, b)$.

Note that since $I(t)$ is bounded for $t \in [0, b)$, there exists $M_1 > 0$ such that $pI(t) < M_1$ for $b > t \geq 0$. Therefore,

$$\frac{dV}{dt} = pI - cV - \gamma AV \leq M_1 - cV, \tag{4.10}$$

which implies that

$$V(t) \leq \max\{V(0), \frac{M_1}{c}\}, \tag{4.11}$$

and, consequently, $V(t)$ is bounded for $t \in [0, b)$.

Let $F_2(t) = B(t) + B_a(t)$. Note that

$$\frac{dF_2}{dt} = -kB_aV - d_BB - d_{B_a}B_a \leq 0. \tag{4.12}$$

Therefore,

$$F_2(t) \leq F_2(0) = B_0 + B_{a0}, \tag{4.13}$$

and, since $B(t)$ and $B_a(t)$ are positive for $t \in [0, b)$, $B(t)$ and $B_a(t)$ are bounded for $t \in [0, b)$.

Note that since $B_a(t)$ and $V(t)$ are bounded for $t \in [0, b)$, there exists $M_2 > 0$ such that $kB_a(t)V(t) < M_2$ for $t \in [0, b)$. Therefore,

$$\begin{aligned} \frac{dP}{dt} =& kB_aV + rP(1 - \frac{P}{K_P}) \\ \leq& M_2 + rP - \frac{r}{K_P}P^2 = \frac{-r}{K_P}(P - X)(P - Y), \end{aligned} \tag{4.14}$$

where

$$\begin{aligned} X &= \frac{K_P + \sqrt{K_P^2 + \frac{4K_PM_2}{r}}}{2}, \\ Y &= \frac{K_P - \sqrt{K_P^2 + \frac{4K_PM_2}{r}}}{2}. \end{aligned} \tag{4.15}$$

Note that $X > 0$, $Y < 0$, and

$$P(t) \leq \frac{X - CYe^{-\frac{r(X-Y)t}{M}}}{1 - Ce^{-\frac{r(X-Y)t}{M}}}, \tag{4.16}$$

where $C = \frac{P_0 - X}{P_0 - Y}$. Therefore $P(t) \leq \max\{P(0), X\}$ for $t \in [0, b)$.

Note that since $P(t)$ is bounded for $t \in [0, b)$, there exists $M_3 > 0$ such that $NP(t) < M_3$ for $t \in [0, b)$. Since

$$\frac{dA}{dt} = NP - d_A A \leq M_3 - d_A A, \tag{4.17}$$

we get that $A(t) \leq \max\{A(0), \frac{M_3}{d_A}\}$. Therefore, $A(t)$ is bounded for $t \in [0, b)$.

This concludes the proof that system (4.1) subject to initial conditions (4.2) has bounded solutions for $t \in [0, b)$. □

Proposition 3. *The solution of system* (4.1) *subject to initial conditions* (4.2) *is positive and bounded for all* $t > 0$.

Proof. In proposition 1 and 2 we showed that the solutions of (4.1) subject to initial conditions (4.2) are positive for all $t \in [0, b)$. This together with the uniform boundedness of solutions on $[0, b)$ implies that $b = \infty$. □

4.1.2 Stability Analysis

In this section we describe model (4.1)'s equilibria and their local stability. System (4.1) has four steady states. The disease-free steady state is given by

$$S_1 = \left(\frac{s}{d_T}, 0, 0, 0, 0, 0, 0\right).$$

The virus persistence in the absence of antibody responses is given by

$$S_2 = (T_2, I_2, V_2, 0, 0, 0, 0).$$

The virus persistence in the presence of antibody responses is given by

$$S_3 = (T_3, I_3, V_3, 0, 0, K_P, K_A).$$

The antibody-induced virus clearance is given by

$$S_4 = \left(\frac{s}{d_T}, 0, 0, 0, 0, K_P, K_A\right),$$

where

$$\begin{aligned} V_2 &= \frac{\beta ps - c\delta d_T}{\beta c\delta}, \\ I_2 &= \frac{\beta ps - c\delta d_T}{\beta p\delta}, \\ T_2 &= \frac{c\delta}{\beta p}, \\ K_A &= \frac{N}{d_A} K_P, \\ T_3 &= \frac{\delta}{\beta p}(1+\eta K_A)(c+\gamma K_A), \\ I_3 &= \frac{s}{\delta} - \frac{d_T}{\beta p}(1+\eta K_A)(c+\gamma K_A), \\ V_3 &= \frac{pI_3}{c+\gamma K_A}. \end{aligned} \tag{4.18}$$

Note that S_2 is positive, and therefore biologically relevant, when

$$R_0 = \frac{\beta ps}{d_T c\delta} > 1. \tag{4.19}$$

R_0 is the basic reproductive number corresponding to a model without antibody responses. It represents the average number of progeny virus generated by one virus over the course of its lifetime, assuming an uninfected monocyte population.

S_3 is positive, and therefore biologically relevant, when

$$R_0^p = \frac{R_0}{(1+\eta K_A)(1+\frac{\gamma}{c}K_A)} > 1. \tag{4.20}$$

R_0^p is the basic reproductive number corresponding to model (4.1) and represents the average number of progeny virus generated by one virus over the course of its lifetime in the presence of strain-specific antibodies, assuming an uninfected monocyte population.

We next study the asymptotic stability of these four steady states.

$$J(\overline{X}) = \begin{pmatrix} -d_T - \frac{\beta V}{1+\eta A} & 0 & -\frac{\beta T}{1+\eta A} & 0 & 0 & 0 & \frac{\beta\eta TV}{(1+\eta A)^2} \\ \frac{\beta V}{1+\eta A} & -\delta & \frac{\beta T}{1+\eta A} & 0 & 0 & 0 & -\frac{\beta\eta TV}{(1+\eta A)^2} \\ 0 & p & -c-\gamma A & 0 & 0 & 0 & -\gamma V \\ 0 & 0 & -\alpha B & -\alpha V - d_B & 0 & 0 & 0 \\ 0 & 0 & \alpha B - kB_a & \alpha V & -d_{B_a} - kV & 0 & 0 \\ 0 & 0 & kB_a & 0 & kV & G & 0 \\ 0 & 0 & 0 & 0 & 0 & N & -d_A \end{pmatrix},$$

is the Jacobian of system (4.1) at the steady state $\overline{X} = S_i$ $(i = 1, ..., 4)$ and $G = r - \frac{2rP}{K_P}$. If all eigenvalues of $J(\overline{X})$ have negative real parts, then the steady state $\overline{X}$ is locally asymptotically stable.

Proposition 4. *Steady state S_1 is unstable.*

Proof. $J(S_1)$ has eigenvalue $\lambda = r > 0$. Therefore S_1 is unstable. □

Proposition 5. *Steady state S_2 is unstable.*

Proof. $J(S_2)$ has eigenvalue $\lambda = r$. Therefore, S_2 is unstable. □

Proposition 6. *Steady state S_3 is locally asymptotically stable when $R_0^p > 1$ and unstable otherwise.*

Proof. $J(S_3)$ has eigenvalues $\lambda_1 = -d_A$, $\lambda_2 = -r$, $\lambda_3 = \frac{kd_T}{\beta}[(1 + \eta K_A) - \frac{\beta ps}{\delta d_T(c+\gamma K_A)}] - d_{B_a}$, $\lambda_4 = \frac{\alpha d_T}{\beta}[(1 + \eta K_A) - \frac{\beta ps}{\delta d_T(c+\gamma K_A)}] - d_B$, which are negative when $R_0^p > 1$. Furthermore, eigenvalues $\lambda_{5,6,7}$ solve

$$\lambda^3 + L_1\lambda^2 + L_2\lambda + L_3 = 0, \tag{4.21}$$

where

$$\begin{aligned} L_1 &= c + \gamma K_A + \delta + \frac{\beta ps}{\delta(1 + \eta K_A)(c + \gamma K_A)}, \\ L_2 &= \frac{\beta ps(c + \gamma K_A + \delta)}{\delta(1 + \eta K_A)(c + \gamma K_A)}, \\ L_3 &= \frac{\beta ps}{(1 + \eta K_A)} - \delta d_T(c + \gamma K_A). \end{aligned} \tag{4.22}$$

By the Routh-Hurwitz condition, λ_5, λ_6, and λ_7 have negative real parts if $L_1 > 0$, $L_3 > 0$ and $D = L_1L_2 - L_3 > 0$. By algebraic manipulation we can show that these relations hold for $R_0^p > 1$. Therefore, the chronic steady state S_3 is locally asymptotically stable if $R_0^p > 1$. □

Proposition 7. *Steady state S_4 is locally asymptotically stable when $R_0^p < 1$ and unstable otherwise.*

Proof. $J(S_4)$ has eigenvalues $\lambda_1 = -d_A$, $\lambda_2 = -d_B$, $\lambda_3 = -d_{B_a}$, $\lambda_4 = -d_T$, $\lambda_5 = -r$ which are always negative, and $\lambda_{6,7}$ given by

$$\lambda^2 + (c + \delta + \gamma K_A)\lambda + \delta(c + \gamma K_A) - \frac{\beta ps}{d_T(1 + \eta K_A)} = 0, \tag{4.23}$$

which have negative real parts if $\delta(c + \gamma K_A) - \frac{\beta ps}{d_T(1+\eta K_A)} > 0$. This is equivalent to $R_0^p < 1$. Therefore, S_4 is locally asymptotically stable if $R_0^p < 1$. □

Note that when S_4 is locally asymptotically stable, S_3 does not exist. Since viral clearance occurs in all instances of dengue infections [37, 38], and this is best described in model (4.1) by the stability of the steady state S_4, we require that $R_0^p < 1$.

4.1.3 Numerical Results

Parameter Values

There are on average $T_0 = 4 \times 10^5$ monocytes per ml of blood in humans [1]. Healthy monocytes die at per capita rate $d_T = 0.01$ per day [6]. We assume that monocytes are at steady-state before virus detection $T_0 = s/d_T$, therefore, $s = 4 \times 10^3$ per ml per day. We assume there is a small number of infected monocytes are the time of virus detection $I_0 = 3 \times 10^{-4}$ per ml. They die at rate $\delta = 3.5$ per day [31]. $V_0 = 357$ RNA per ml, corresponding to the limit of detection [39]. Virus is produced at rate $p = 6.7 \times 10^3$ per infected cell per day [22] and cleared at rate $c = 5$ per day, higher than the death rate of infected cells. We will investigate the effects of varying the clearance rate.

There are $B_0 = 2 \times 10^6$ B-cells per ml in human blood [1]. We assume there are no dengue-specific activated B cells, plasma cells or antibodies at the time of virus detection, $B_{a0} = 0$, $P_0 = 0$ and $A_0 = 0$. Resting and activated B cells die at rates $d_B = d_{B_a} = 0.2$ per day [35]. Plasma cells proliferate at rate $r = 1$ per day [27, 35] and reach a carrying capacity $K_P = 1.3 \times 10^4$ cells per ml. Antibodies are produced at a rate of $N = 10^8$ per plasma cell per day [1] and die at rate $d_A = 0.07$ per day [44].

For the unknown parameters $\{\beta, \alpha, \eta, k, \gamma\}$ we use $\beta = 2.4 \times 10^{-8}$ ml per virus per day, $\alpha = 10^{-15}$ ml per virus per day, $\eta = 3 \times 10^{-7}$ ml per antibody, $k = 10^{-5}$ ml per virus per day, $\gamma = 8 \times 10^{-10}$ ml per antibody per day. To determine these values, we assume that primary infection results in dengue fever with a viral peak of approximately 5×10^7 virus per ml [37]. Also, we assume that dengue virus is cleared regardless of the disease severity [11] (therefore S_4 is stable, *i.e.*, $R_0^p < 1$) and virus is cleared by day 7 [11]. Since all three assumptions hold when these parameter values are chosen and the numbers appear to be biologically reasonable, we choose these values for the unknown parameters. The parameter values are summarized in Table 4.1.

Table 4.1: Fixed parameters used in simulations.

Initial Condition	Description	Value	Units	Reference
T_0	Initial uninfected monocytes	4×10^5	cells/ml	[1]
I_0	Initial infected monocytes	3×10^{-4}	cells/ml	-
V_0	Initial virus	357	RNA/ml	[39]
B_0	Initial naive B-cells	2×10^6	cells/ml	[1]
B_{a0}	Initial activated B-cells	0	cells/ml	-
P_0	Initial plasma cells	0	cells/ml	-
A_0	Initial antibody	0	molecules/ml	-
Parameter	Description	Value	Units	Reference
s	Uninfected monocytes production rate	4×10^3	cells/ml $\cdot$ day	[6]
d_T	Uninfected monocytes death rate	0.01	per day	[6]
β	Infectivity rate	2.4×10^{-8}	ml/RNA $\cdot$ day	-
η	Antibody neutralization rate	3×10^{-7}	ml/molecules	-
δ	Infected monocytes death rate	3.5	per day	[31]
p	Virus production rate	6.7×10^3	per day	[22]
c	Virus clearance rate	5	per day	-
γ	Strain-specific antibody non-neutralization effect	8×10^{-10}	ml/molecules $\cdot$ day	-
α	B-cell activation rate	10^{-15}	ml/RNA $\cdot$ day	-
d_B	Naive B-cells death rate	0.2	per day	[35]
d_{B_a}	Activated B-cells death rate	0.2	per day	[35]
k	Plasma cells recruitment	10^{-5}	ml/RNA $\cdot$ day	-
r	Plasma cells division rate	1	per day	[35]
K_P	Plasma cells carrying capacity	1.3×10^4	cells/ml	-
N	Antibody production rate	10^8	molecules/cells $\cdot$ day	[1]
d_A	Antibody death rate	0.07	per day	[44]
τ	Second virus time of detection	500	days	

The dynamics of model (4.1) and parameters in Table 4.1 are presented in Fig. 4.1. Our model predicts that the maximum virus density of 7.7×10^7 per ml is reached 3.9 days following virus detection. These predictions are similar to values and timing observed during primary dengue fever infection [11, 38]. Moreover, we predict that the virus decays below its limit of detection of 357 RNA per ml 8.7 days later, consistent with clinical observations [36] (see Fig. 4.1b).

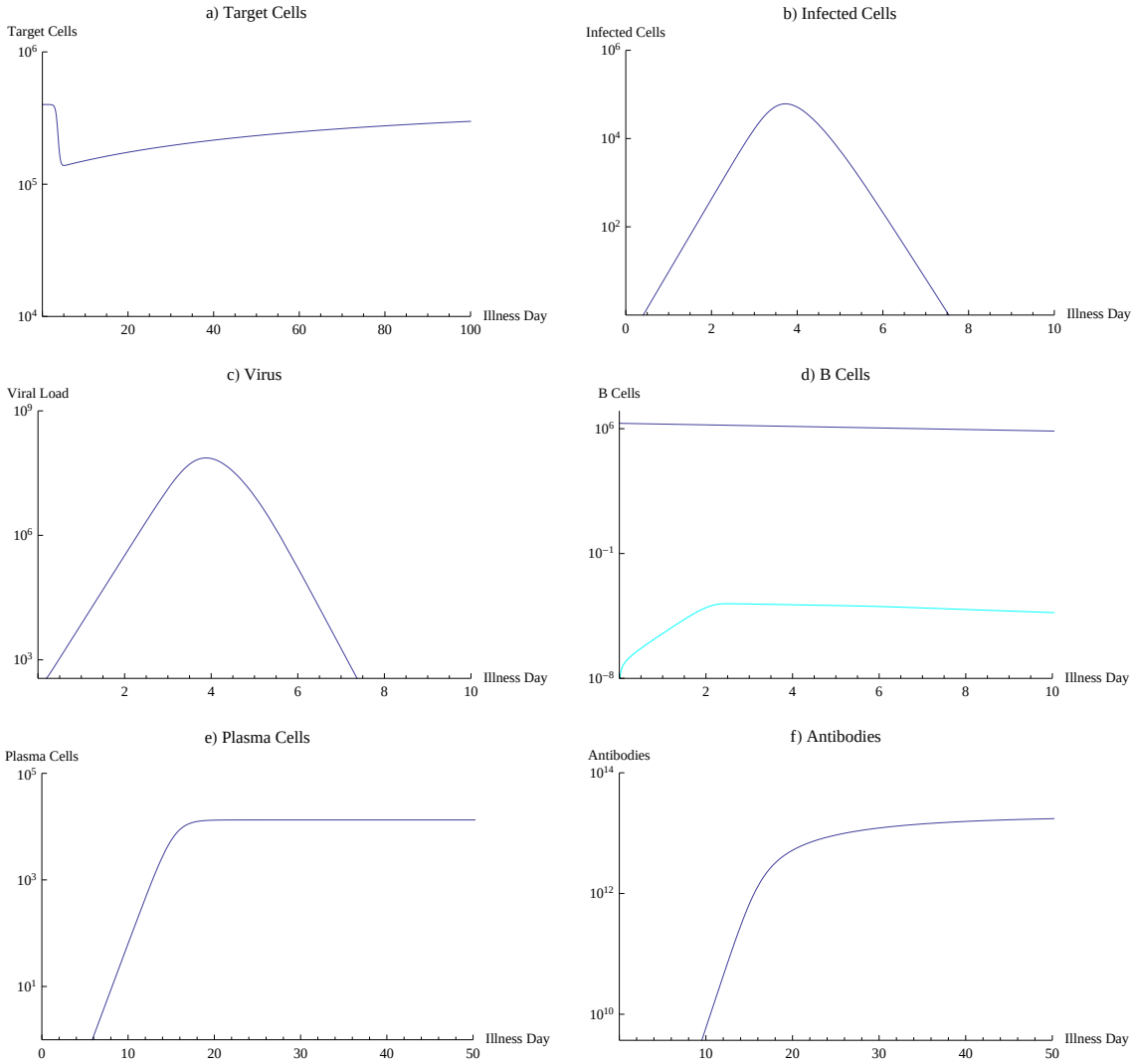

Figure 4.1: Dynamics of primary infection.

The model predicts a slow initial antibody growth with free antibodies rising above their limit of detection of 1 ng/ml (3.7×10^9 molecules per ml) [8] approximately 9.5 days following virus detection. At this time the viremia is resolved, and the virus is below the level of detection. This result is consistent with the reported appearance of IgM and IgG antibodies after virus resolution, approximately 1 to 2 weeks after infection [2]. Antibodies reach their carrying capacity $K_A = 5.1$ μg per ml (1.9×10^{13} molecules per ml) approximately 471 days after virus infection, consistent with experimental findings [12] (see Fig. 4.1d).

4.1.4 Sensitivity Analysis

For the estimated parameters β, c, γ and η mentioned above, we want to determine the effect on the solution when these parameters are changed slightly. Since these parameters are unknown and have yet to be discovered biologically, it is important to understand their relationship to the simulation. Using the method of sensitivity analysis [4], we can determine the effect of a parameter on the solution mathematically rather than running many simulations and varying a specific parameter each time. For each solution in a system and an arbitrary parameter q, we treat the solution as a function of time and of the parameter. We consider the sensitivity functions by taking the partial derivative of the solution with respect to the parameter q. So, for the system 4.1, the sensitivity functions are

$$\begin{aligned} T_q &= \frac{\partial T(t,q)}{\partial q} \\ I_q &= \frac{\partial I(t,q)}{\partial q} \\ V_q &= \frac{\partial V(t,q)}{\partial q} \\ B_q &= \frac{\partial B(t,q)}{\partial q} \\ B_{a_q} &= \frac{\partial B_a(t,q)}{\partial q} \\ P_q &= \frac{\partial P(t,q)}{\partial q} \\ A_q &= \frac{\partial A(t,q)}{\partial q} \end{aligned} \tag{4.24}$$

The value of these functions at a specific time t represent the rate of change in the original function with respect to the specific parameter. For example, if we plot qV_q, known as the semi-relative sensitivity solution, and evaluate it at a specific time t, we can determine how much the viral load will change at time t if the parameter q is doubled. However, to find V_q, we must use the system 4.1 and take the partial derivative with respect to q of each function. For example, the sensitivity system with respect to β is

$$
\begin{aligned}
\frac{dT_\beta}{dt} &= -\frac{\beta T_\beta V + \beta V_\beta T + TV}{1+\eta A} + \frac{\beta \eta TV A_\beta}{(1+\eta A)^2} - d_T T_\beta, \\
\frac{dI_\beta}{dt} &= \frac{\beta T_\beta V + \beta V_\beta T + TV}{1+\eta A} - \frac{\beta \eta TV A_\beta}{(1+\eta A)^2} - \delta I_\beta, \\
\frac{dV_\beta}{dt} &= pI_\beta - cV_\beta - \gamma V_\beta A - \gamma V A_\beta, \\
\frac{dB_\beta}{dt} &= -\alpha B_\beta V - \alpha B V_\beta - d_B B_\beta, \\
\frac{dB_{a_\beta}}{dt} &= \alpha B_\beta V + \alpha B V_\beta - k B_{a_\beta} V - k B_a V_\beta - d_{B_a} B_{a_\beta}, \\
\frac{dP_\beta}{dt} &= rP_\beta - 2\frac{r}{K_P} P P_\beta + k B_{a_\beta} V + k B_a V_\beta, \\
\frac{dA_\beta}{dt} &= NP_\beta - d_A A_\beta.
\end{aligned}
\tag{4.25}
$$

We then combine the sensitivity system and the original system into one system and use the parameters in Table 4.1 along with $T_q(0) = I_q(0) = V_q(0) = B_q(0) = B_{a_q} = P_q = A_q = 10^{-6}$. Small initial conditions are used since it is assumed that changing a parameter does not drastically affect the solution close to the initial time. By solving this new system, we can determine the effect of the parameter q on the various solutions.

Using the above process, we can plot βV_β to determine how much doubling the parameter of β affects the viral load.

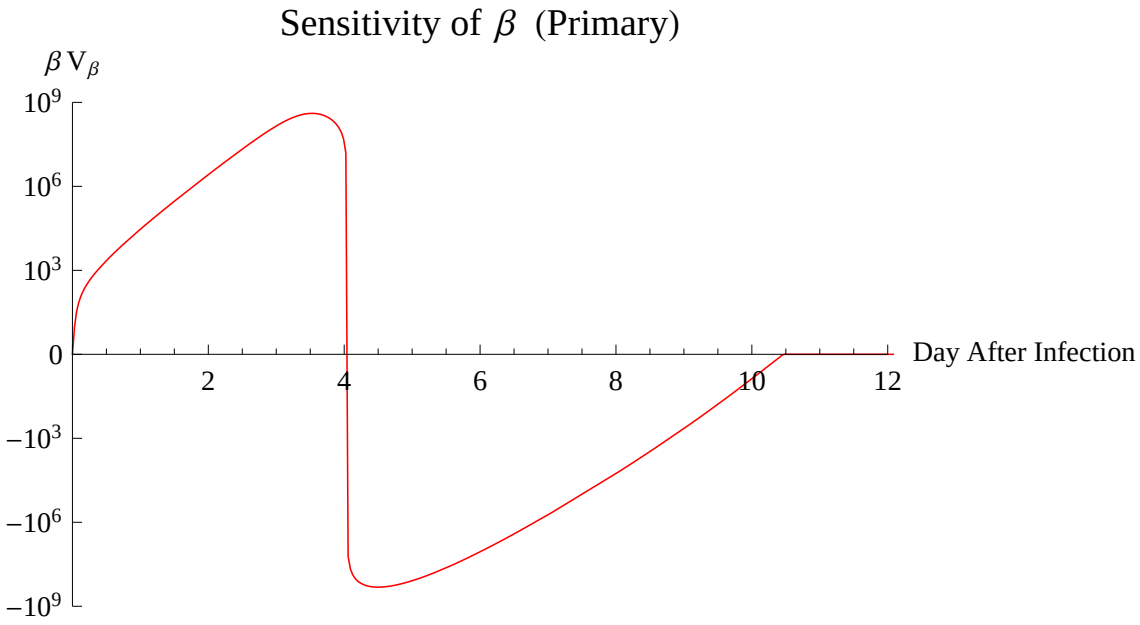

Figure 4.2: Sensitivity of the primary infection model with respect to β.

In Fig 4.2, we see that if the parameter is doubled at time $t = 4$, we have that the peak of the virus is shifted towards the left due to the negative effect of β after this point.

We can now perform the sensitivity analysis on the other parameters and plot the graphs of qV_q. The sensitivity system with respect to c is

$$\begin{aligned}
\frac{dT_c}{dt} &= -\frac{\beta T_c V + \beta T V_c}{1+\eta A} + \frac{\beta\eta T V A_c}{(1+\eta A)^2} - d_T T_c,\\
\frac{dI_c}{dt} &= \frac{\beta T_c V + \beta T V_c}{1+\eta A} - \frac{\beta\eta T V A_c}{(1+\eta A)^2} - \delta I_c,\\
\frac{dV_c}{dt} &= pI_c - cV_c - V - \gamma V_c A - \gamma V A_c,\\
\frac{dB_c}{dt} &= -\alpha B_c V - \alpha B V_c - d_B B_c,\\
\frac{dB_{a_c}}{dt} &= \alpha B_c V + \alpha B V_c - kB_{a_c} V - kB_a V_c - d_{B_a} B_{a_c},\\
\frac{dP_c}{dt} &= rP_c - \frac{r}{K_P} P P_c + kB_{a_c} V + kB_a V_c,\\
\frac{dA_c}{dt} &= NP_c - d_A A_c.
\end{aligned} \tag{4.26}$$

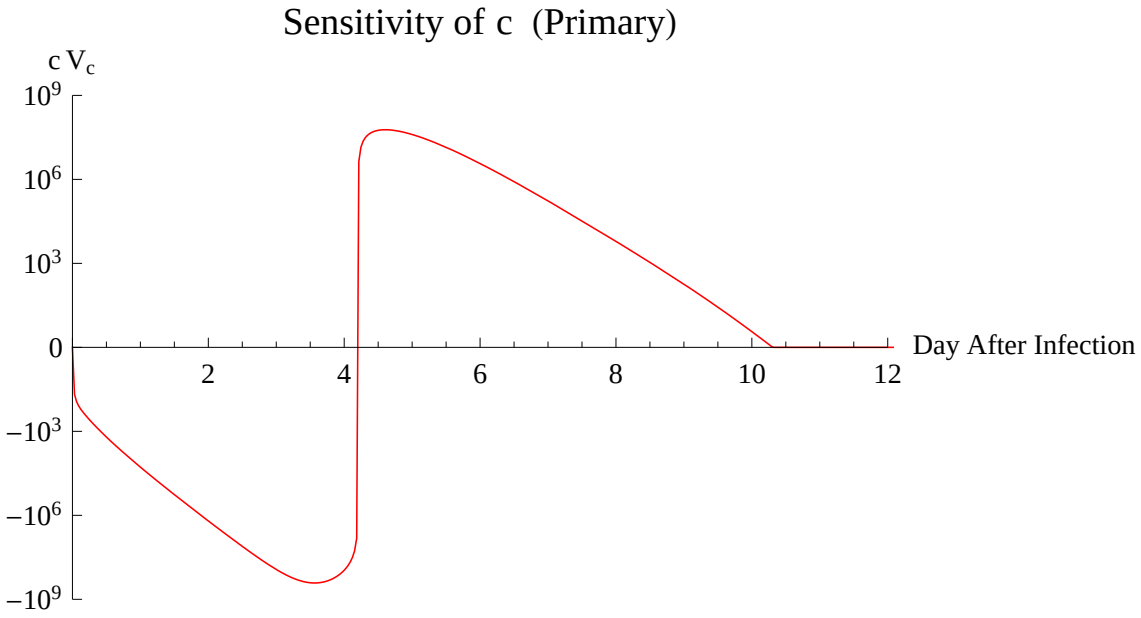

Figure 4.3: Sensitivity of the primary infection model with respect to c.

From studying the graph of cV_c in Fig 4.3, we find that c has the opposite effect of β, since if c is doubled at time $t = 4$, then the virus peak will be shifted towards the right due to the positive effect from c after this point.

The sensitivity system with respect to γ is

$$\begin{aligned}
\frac{dT_\gamma}{dt} &= -\frac{\beta T_\gamma V + \beta T V_\gamma}{1+\eta A} + \frac{\beta\eta T V A_\gamma}{(1+\eta A)^2} - d_T T_\gamma,\\
\frac{dI_\gamma}{dt} &= \frac{\beta T_\gamma V + \beta T V_\gamma}{1+\eta A} - \frac{\beta\eta T V A_\gamma}{(1+\eta A)^2} - \delta I_\gamma,\\
\frac{dV_\gamma}{dt} &= pI_\gamma - cV_\gamma - \gamma V_\gamma A - \gamma V A_\gamma - VA,\\
\frac{dB_\gamma}{dt} &= -\alpha B_\gamma V - \alpha B V_\gamma - d_B B_\gamma,\\
\frac{dB_{a_\gamma}}{dt} &= \alpha B_\gamma V + \alpha B V_\gamma - kB_{a_\gamma} V - kB_a V_\gamma - d_{B_a} B_{a_\gamma},\\
\frac{dP_\gamma}{dt} &= rP_\gamma - \frac{r}{K_P} P P_\gamma + kB_{a_\gamma} V + kB_a V_\gamma,\\
\frac{dA_\gamma}{dt} &= NP_\gamma - d_A A_\gamma.
\end{aligned} \tag{4.27}$$

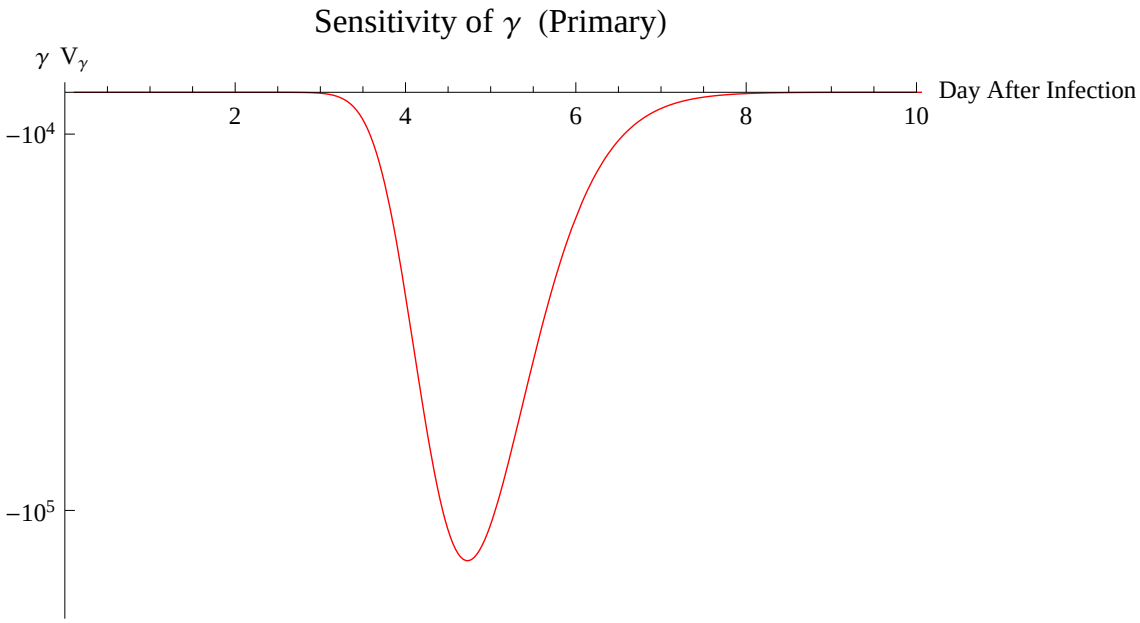

Figure 4.4: Sensitivity of the primary infection model with respect to γ.

From studying the graph of γV_γ in Fig 4.4, we find that γ has a negative effect on the virus. This makes sense since γ is the rate of enhancement of the viral clearance by the antibodies.

$$\begin{aligned}
\frac{dT_\eta}{dt} &= -\frac{\beta T_\eta V + \beta T V_\eta}{1+\eta A} + \frac{\beta\eta T V A_\eta + \beta T V A}{(1+\eta A)^2} - d_T T_\eta, \\
\frac{dI_\eta}{dt} &= \frac{\beta T_\eta V + \beta T V_\eta}{1+\eta A} - \frac{\beta\eta T V A_\eta + \beta T V A}{(1+\eta A)^2} - \delta I_\eta, \\
\frac{dV_\eta}{dt} &= pI_\eta - cV_\eta - \gamma V_\eta A - \gamma V A_\eta, \\
\frac{dB_\eta}{dt} &= -\alpha B_\eta V - \alpha B V_\eta - d_B B_\eta, \\
\frac{dB_{a_\eta}}{dt} &= \alpha B_\eta V + \alpha B V_\eta - k B_{a_\eta} V - k B_a V_\eta - d_{B_a} B_{a_\eta}, \\
\frac{dP_\eta}{dt} &= rP_\eta - \frac{r}{K_P} P P_\eta + k B_{a_\eta} V + k B_a V_\eta, \\
\frac{dA_\eta}{dt} &= N P_\eta - d_A A_\eta.
\end{aligned} \tag{4.28}$$

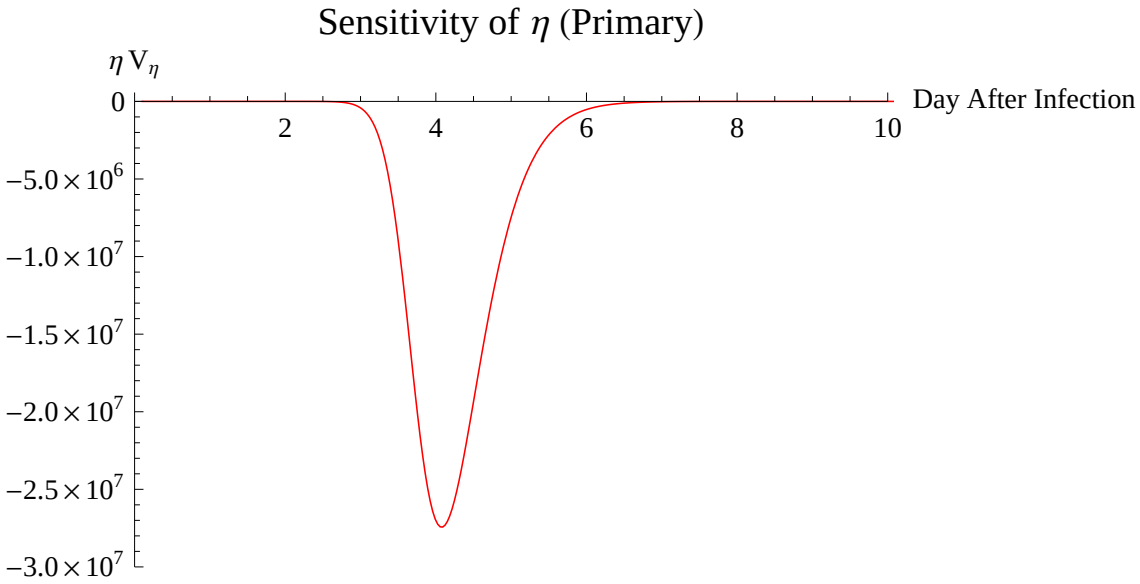

Figure 4.5: Sensitivity of the primary infection model with respect to η.

From studying the graph of ηV_η in Fig 4.5, we find that η has a negative effect on the virus. This also makes sense since η is the reduction rate of the viral infectivity by antibodies. As compared to γ, we find that η has a larger negative effect than γ, which means neutralizing antibodies have more of an effect than non-neutralizing antibodies in clearing virus as a result of primary infection.

4.2 Secondary Infections

Following primary dengue infection, virus is eliminated and long-lived plasma cells and antibodies specific to the strain persist in the body. This is described in model (4.1) by the stability of S_4, with plasma cells and the antibodies at their carrying capacities, K_P and K_A. If the patient is reinfected with a different virus serotype both strain-specific and cross-reactive antibodies develop. We model the host-second virus interactions in a manner similar to the response to the primary infection. The difference consists in the interaction between pre-existing antibodies specific to the first virus and the second virus strain. As stated in Chapter 2, cross-reactive antibodies bind to the second virus strain, form immune complexes, but do not neutralize the heterologous virus [41]. Instead, monocytes that bind to the Fc-region of such complexes ingest the virus and get infected in the process. This leads to an antibody-dependent enhancement of infection. Since we model two antibody functions, one that reduces infectivity and one that enhances virus clearance, we investigate the effect of cross-reactive antibody in disease enhancement as follows. We assume that the infectivity

rate of virus V_2 is enhanced by the presence of cross-reactive antibodies, *i.e.* $\beta_2 = \beta_1(1+\xi A_1)$, and is reduced, as before, by its specific antibody A_2 at rate $\eta_2 = \eta_1 = \eta$. Since we assume that the antibody to the first virus reached its carrying capacity at the time of second infection, the second virus infectivity rate is constant over time, *i.e.*, $\beta_2 = \beta_1(1 + \xi K_A)$=const. As before, we assume that antibodies enhance the clearance of their specific virus i at rate γ_i $(i = 1, 2)$. However, the cross-reactive antibody A_1 interferes with the clearance of the second virus V_2 by rendering it unavailable to strain-specific antibody binding. We model this phenomena as reduction of V_2 clearance at rate $\gamma_E A_1$. For simplicity, we assume $\gamma_2 > \gamma_E$. Lastly, we assume that the production rate of the second virus is greater than that of the first virus $p_2 > p_1$, as reported experimentally [22]. The new model is

$$\begin{aligned}
\frac{dT}{dt} &= s - d_T T - \frac{\beta_1 T V_1}{1+\eta A_1} - \frac{\beta_2 T V_2}{1+\eta A_2},\\
\frac{dI_i}{dt} &= \frac{\beta_i T V_i}{1+\eta A_i} - \delta I_i,\\
\frac{dV_1}{dt} &= p_1 I_1 - (c + \gamma_1 A_1) V_1,\\
\frac{dV_2}{dt} &= p_2 I_2 - (c + \gamma_2 A_2 - \gamma_E A_1) V_2,\\
\frac{dB}{dt} &= -\alpha B V_1 - \alpha B V_2 - d_B B,\\
\frac{dB_{a_i}}{dt} &= \alpha B V_i - k B_{a_i} V_i - d_{B_a} B_{a_i},\\
\frac{dP_i}{dt} &= r P_i (1 - \frac{P_i}{K_P}) + k B_{a_i} V_i,\\
\frac{dA_i}{dt} &= N P_i - d_A A_i,
\end{aligned} \tag{4.29}$$

where $i = 1, 2$. The initial conditions at day τ, corresponding to the detection time of the second virus, are

$$\begin{aligned}
&T(\tau) = s/d_T > 0, I_1(\tau) = 0, I_2(\tau) = I_0, V_1(\tau) = 0, V_2(\tau) = V_0, B(\tau) = B_0,\\
&B_{ai}(\tau) = 0, P_1(\tau) = K_P, P_2(\tau) = 0, A_1(\tau) = K_A, A_2(\tau) = 0,
\end{aligned} \tag{4.30}$$

where $i = 1, 2$.

4.2.1 Analytical Results

Proposition 8. *System* (4.29) *subject to positive initial conditions has positive solutions for all* $t > \tau$.

Proof. The proof is similar with the proof of Proposition 1.

Proposition 9. *System* (4.29) *subject to positive initial conditions has bounded solutions for all* $t > \tau$.

Proof. The proof is similar with the proof of Proposition 2.

4.2.2 Stability Analysis

We investigate model (4.29) under the assumption that the patient has cleared the primary dengue virus infection, *i.e.*, steady state S_4 is locally asymptotically stable. Therefore

$$R_0^p = \frac{\beta_1 p_1 s}{d_T c \delta (1+\eta K_A)(1+\frac{\gamma_1}{c}K_A)} < 1.$$

Under these conditions system (4.29) has four steady states

$$\begin{aligned}
S_5 &= (\frac{s}{d_T}, 0, 0, 0, 0, 0, 0, 0, 0, K_P, 0, K_A, 0),\\
S_6 &= (T_6, 0, I_6, 0, V_6, 0, 0, 0, K_P, 0, K_A, 0),\\
S_7 &= (T_7, 0, I_7, 0, V_7, 0, 0, 0, K_P, K_P, K_A, K_A),\\
S_8 &= (\frac{s}{d_T}, 0, 0, 0, 0, 0, 0, 0, K_P, K_P, K_A, K_A),
\end{aligned} \tag{4.31}$$

where

$$\begin{aligned}
T_6 &= \frac{\delta(c-\gamma_E K_A)}{\beta_2 p_2},\\
I_6 &= \frac{\beta_2 p_2 s - \delta d_T (c-\gamma_E K_A)}{\delta \beta_2 p_2},\\
V_6 &= \frac{\beta_2 p_2 s - \delta d_T (c-\gamma_E K_A)}{\beta_2 \delta (c-\gamma_E K_A)},\\
T_7 &= \frac{\delta(1+\eta K_A)(c+(\gamma_2-\gamma_E)K_A)}{\beta_2 p_2},\\
I_7 &= \frac{\beta_2 p_2 s - \delta d_T (1+\eta K_A)(c+(\gamma_2-\gamma_E)K_A)}{\delta \beta_2 p_2},\\
V_7 &= \frac{\beta_2 p_2 s - \delta d_T (1+\eta K_A)(c+(\gamma_2-\gamma_E)K_A)}{\beta_2 \delta (c+(\gamma_2-\gamma_E)K_A)}.
\end{aligned} \tag{4.32}$$

Let $J_2(\overline{X})$ be the Jacobian of (4.29) at steady state $\overline{X}$.

$$J(\overline{X}) = \begin{pmatrix} J_1 & J_2 & O_{5\times5} & J_3 \\ O_{7\times3} & J_4 & & J_5 \end{pmatrix}$$

where $O_{m\times n}$ is a zero matrix of m rows by n columns and

$$J_1 = \begin{pmatrix} -dT - \frac{\beta_1 V_1}{1+A_1\eta} - \frac{\beta_2 V_2}{1+A_2\eta} & 0 & 0 \\ \frac{\beta_1 V_1}{1+A_1\eta} & -\delta & 0 \\ \frac{\beta_2 V_2}{1+A_2\eta} & 0 & -\delta \\ 0 & p_1 & 0 \\ 0 & 0 & p_2 \end{pmatrix} \quad J_2 = \begin{pmatrix} -\frac{\beta_1 T}{1+A_1\eta} & -\frac{\beta_2 T}{1+A_2\eta} \\ \frac{\beta_1 T}{1+A_1\eta} & 0 \\ 0 & \frac{\beta_2 T}{1+A_2\eta} \\ -c - A_1\gamma_1 & 0 \\ 0 & -c + A_1\gamma_E - A_2\gamma_2 \end{pmatrix}$$

$$J_3 = \begin{pmatrix} \frac{\beta_1\eta T V_1}{(1+\eta A_1)^2} & \frac{\beta_2\eta T V_2}{(1+\eta A_2)^2} \\ \frac{-\beta_1\eta T V_1}{(1+\eta A_1)^2} & 0 \\ 0 & \frac{-\beta_2\eta T V_2}{(1+\eta A_2)^2} \\ -\gamma_1 V_1 & 0 \\ \gamma_E V_2 & -\gamma_2 V_2 \end{pmatrix} \quad J_4 = \begin{pmatrix} -\alpha B & -\alpha B \\ \alpha B - kB_{a_1} & 0 \\ 0 & \alpha B - kB_{a_2} \\ kB_{a_1} & 0 \\ 0 & kB_{a_2} \\ 0 & 0 \\ 0 & 0 \end{pmatrix}$$

$$J_5 = \begin{pmatrix} -d_B - \alpha V_1 - \alpha V_2 & 0 & 0 & 0 & 0 & 0 & 0 \\ \alpha V_1 & -d_{B_a} - kV_1 & 0 & 0 & 0 & 0 & 0 \\ \alpha V_2 & 0 & -d_{B_a} - kV_2 & 0 & 0 & 0 & 0 \\ 0 & kV_1 & 0 & r - 2r\frac{P_1}{K_P} & 0 & 0 & 0 \\ 0 & 0 & kV_2 & 0 & r - 2r\frac{P_2}{K_P} & 0 & 0 \\ 0 & 0 & 0 & N & 0 & -d_A & 0 \\ 0 & 0 & 0 & 0 & N & 0 & -d_A \end{pmatrix}$$

Proposition 10. *Steady state S_5 is unstable.*

Proof. By analyzing $J_2(S_5)$, we find that one eigenvalue is $\lambda_1 = r > 0$, which implies S_5 is unstable. □

Proposition 11. *Steady state S_6 is unstable.*

Proof. By analyzing $J_2(S_6)$, we find that one eigenvalue is $\lambda_1 = r > 0$, which implies S_6 is unstable. □

Proposition 12. *Steady state S_7 is locally asymptotically stable when*

$$R_0^s = \frac{R_{02}}{(1+\eta K_A)(1+\frac{\gamma_2-\gamma_E}{c}K_A)} > 1, \tag{4.33}$$

where $R_{02} = \frac{\beta_2 p_2 s}{d_T c\delta}$ and unstable otherwise.

Proof. Note that S_7 exists when $V_7 > 0$, which is equivalent to $R_0^s > 1$. The Jacobian $J_2(S_7)$ has eigenvalues $\lambda_1 = -d_{B_a}$, $\lambda_{2,3} = -d_A$, $\lambda_{4,5} = -r$, which are always negative. Eigenvalues

$\lambda_6 = -d_B - \frac{\alpha d_T(1+\eta K_A)}{\beta_2}(R_0^s - 1)$, $\lambda_7 = -d_{B_a} - \frac{k d_T(1+\eta K_A)}{\beta_2}(R_0^s - 1)$ are negative when $R_0^s > 1$. Eigenvalues λ_8 and λ_9 solve

$$\lambda^2 + (c + \delta + \gamma_1 K_A)\lambda + L_1 = 0,$$

where

$$L_1 = c\delta(1 + \frac{\gamma_1}{c}K_A)(1 + \eta K_A)\left(1 - \frac{R_0^p}{R_0^s}\right). \tag{4.34}$$

Since we assumed that $R_0^p < 1$ and $R_0^s > 1$, $L_1 > 0$. Consequently, $\lambda_{8,9}$ have negative real parts.

Finally, λ_{10}, λ_{11} and λ_{12} solve

$$\lambda^3 + L_2\lambda^2 + L_3\lambda + L_4 = 0,$$

where

$$\begin{aligned}
L_2 &= c + d_T + \delta + K_A(\gamma_2 - \gamma_E) + \frac{\beta_2 p_2 s - \delta d_T(\eta K_A + 1)((\gamma_2 - \gamma_E)K_A + c)}{\delta(\eta K_A + 1)(c + (\gamma_2 - \gamma_E)K_A)}, \\
L_3 &= \frac{\beta_2 p_2 s + \delta(c + \delta)(c + (\gamma_2 - \gamma_E)K_A)}{\delta(1 + \eta K_A)(c + (\gamma_2 - \gamma_E)K_A)}, \\
L_4 &= (c + \delta)\frac{\beta_2 p_2 s - \delta d_T(1 + \eta K_A)(c + (\gamma_2 - \gamma_E)K_A)}{\delta(1 + \eta KA)(c + (\gamma_2 - \gamma_E)K_A)}.
\end{aligned} \tag{4.35}$$

By the Routh-Hurwitz conditions, λ_{10}, λ_{11}, and λ_{12} have negative real parts if $L_2 > 0$, $L_4 > 0$, and $D = L_2 L_3 - L_4 > 0$. By algebraic manipulation, we can show that these inequalities hold when $R_0^s > 1$. Therefore, steady state S_7 is locally asymptotically stable when $R_0^s > 1$. □

Proposition 13. *The steady state S_8 is locally asymptotically stable when $R_0^s < 1$ and unstable otherwise.*

Proof. $J_2(S_8)$ has eigenvalues $\lambda_{1,2} = -d_A$, $\lambda_3 = -d_B$, $\lambda_{4,5} = -d_{B_a}$, $\lambda_6 = -d_T$, $\lambda_{7,8} = -r$ which are always negative. λ_9 and λ_{10} solve

$$\lambda^2 + (c + \delta + \gamma_1 K_A)\lambda + L_1 = 0,$$

where

$$L_1 = \delta c(1 + \frac{\gamma_1}{c}K_A)(1 - R_0^p). \tag{4.36}$$

Since $L_1 > 0$ when $R_0^p < 1$, eigenvalues $\lambda_{9,10}$ have negative real parts.

Finally, λ_{11} and λ_{12} solve

$$\lambda^2 + L_2\lambda + L_3 = 0,$$

where

$$L_2 = (\gamma_2 - \gamma_E)K_A + c + \delta \tag{4.37}$$

and

$$L_3 = c\delta(1 + \frac{\gamma_2 - \gamma_E}{c}K_A)(1 - R_0^s). \tag{4.38}$$

Since $L_3 > 0$ when $R_0^s < 1$, $\lambda_{11,12}$ have negative real parts. Therefore, S_8 is locally asymptotically stable when $R_0^s < 1$. □

As in the case of the primary infection, the virus is always cleared [37, 38]. This is best described in model (4.29) by the stability of the steady state S_8. Therefore we require that $R_0^s < 1$.

R_0^s is the basic reproductive number corresponding to model (4.29) and represents the average number of progeny virus generated by one virus over the course of its lifetime in the presence of cross-reactive antibodies, assuming an uninfected monocyte population.

When $p_1 = p_2$, $\gamma_1 = \gamma_2$, antibody dependent enhancement does not occur, *i.e.*, $\beta_2 = \beta_1$, $\gamma_E = 0$, and $R_0^s = R_0^p$. If however, the heterologous antibodies enhance the infection, then $\beta_2 > \beta_1$ and/or $\gamma_E > 0$, along with $R_0^s > R_0^p$.

4.2.3 Numerical Results

Homologous Infections

If the patient is reinfected with the same virus serotype, the immune response and virus elimination is faster due to the presence of pre-existing antibodies (which we assumed reached their carrying capacity, $A_1 = K_A$). We model homologous secondary infections by assuming system (4.1) is subject to initial conditions

$$(T, I, V, B, B_a, P, A)(\tau) = \left(\frac{s}{d_T}, I_0, V_0, B_0, 0, K_P, K_A\right), \tag{4.39}$$

where τ represents the detection time of second virus. The long-term outcomes are identical to those of model (4.1). Using $\tau = 500$, we see in Fig. 4.6 that the virus is rapidly eliminated without creating viremia, consistent with lifelong immunity from the same virus serotype.

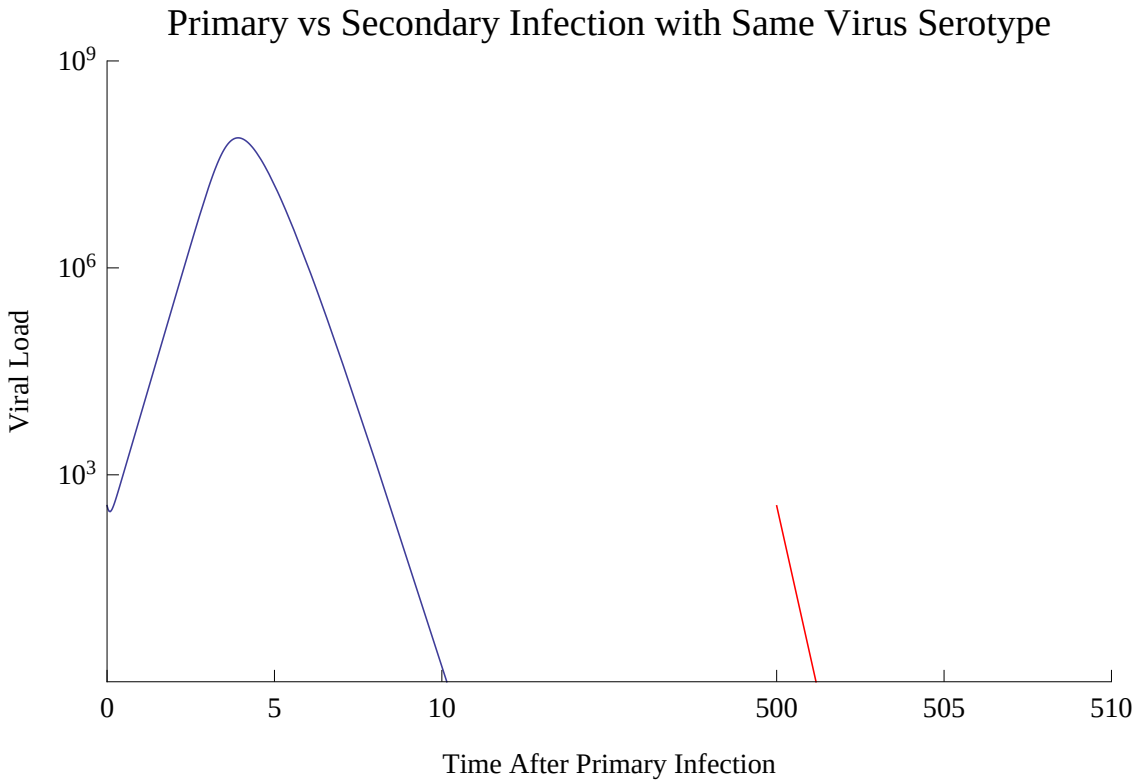

Figure 4.6: Secondary infection with a homologous serotype.

Data fitting

We aim to map the differences between the virus-host interactions in secondary DF and DHF as a result of heterologous infections. We fit V_2 as given by model (4.29) with initial conditions (4.30) to patient data. We use the total viral load as measured from secondary infection-induced DF and DHF published by Wang et al. (Figs 4.7 A and B). We define the time course as follows. In our model, $t = \tau$ corresponds to time of secondary virus detection and the first data points in DF and DHF cases in Wang et al. [39] correspond to three days after τ in our model.

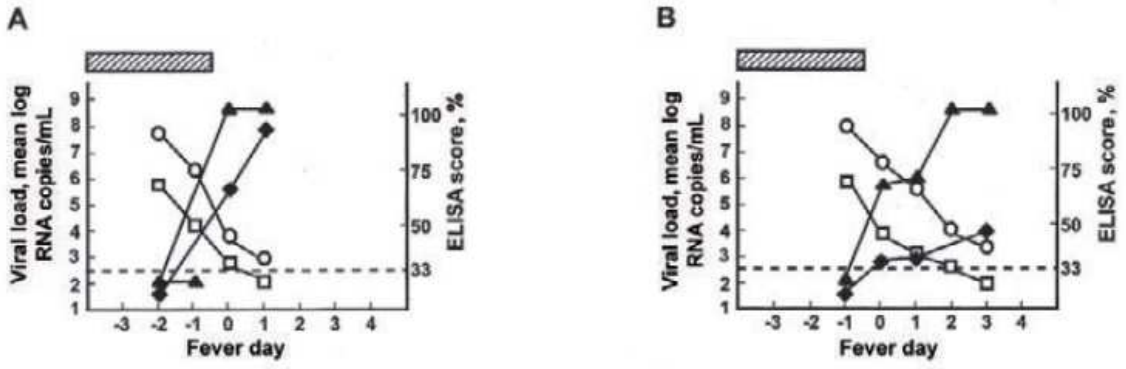

Figure 4.7: Secondary infection data for patients with DF (A) and DHF (B) [39].

We assume that all shared parameter values are equal to their values in primary infection (see Table 4.1) and use the data to estimate the production and infectivity rates of the heterologous virus, p_2 and β_2, the strain-specific antibody-mediated clearance rate of heterologous virus γ_2, and the cross-reactive antibody-induced decrease in heterologous virus clearance rate γ_E. We denote β_2^{DHF} and β_2^{DF} as the second virus infectivity rates resulting in DHF and DF, respectively. We start with the assumption that $\beta_2 > \beta_1$ and $\beta_2^{DHF} > \beta_2^{DF}$ (to account for antibody induced enhancement), $p_2 > p_1$ (to account for higher virus production during secondary infections [22]) and $\gamma_E > 0$ (to account for decreased virus clearance during secondary infections [39]). We use the 'fminsearch' algorithm in Matlab.

ADE as a Result of Neutralizing Antibodies

We first assume that only neutralizing antibodies enhance secondary infection through antibody-dependent enhancement. If neutralizing antibodies play a role in secondary infection, more host cells are susceptible to infection as described in chapter two. Thus, the infectivity rate is higher for more severe infection. So, we attempt to fit the data such that $p_2 = p_1$, $\gamma_2 = \gamma_1$, $\gamma_E = 0$, $\beta_2 > \beta_1$ and $\beta_2^{DHF} > \beta_2^{DF}$. For $\beta_2 = \beta_1(1 + \xi K_A)$, we obtain that $\xi^{DF} = -.2$ and $\xi^{DHF} = -.6$. This implies that $\beta_2^{DHF} < \beta_2^{DF} < \beta_1$.

When comparing secondary DF and DHF, we should have that the viral peak of DHF is higher [37], the viral clearance time of DHF is later [39], and the viral peak times are similar [36]. However, in this case, the viral peak of DHF is lower than the viral peak in DF and the viral peak time of DHF is later, which is inconsistent with these dynamics. These results suggest that the pre-existing antibodies either do not enhance infectivity, or that increased infectivity observed during DHF is compensated by increased clearance. Therefore, we assume that the cross-reactive antibody does not lead to enhancement of virus infectivity and set $\beta_2 = \beta_1$.

Enhancement as a Result of Non-Neutralizing Antibodies

Due to the results from the our first attempt at fitting, we assume that enhancement occurs as a result of the interaction between non-neutralizing antibodies from primary infection and virus from the secondary infection. Thus, we fit the parameters $\{p_2, \gamma_2, \gamma_E\}$ since these parameters correspond to the effect on the virus from non-neutralizing antibodies. The results are presented in Tables 4.2 and 4.3 and the best fits are presented in Figs. 4.8 and 4.9.

Table 4.2: Best parameters obtained by fitting (4.29) to patient data.

	Disease Level	p_2	γ_2	γ_E	RSS
a	DF	2×10^4	7×10^{-10}	7.4×10^{-15}	1.89
b	DHF	2×10^4	2.1×10^{-11}	1.6×10^{-13}	1.85

Table 4.3: Confidence intervals obtained by fitting (4.29) to patient data.

Disease Level	Parameter	Interval
DF	p_2	$(1.3 \times 10^4, 2.6 \times 10^4)$
DF	γ_2	$(-1.5 \times 10^{-9}, 2.9 \times 10^{-9})$
DF	γ_E	$(4.9 \times 10^{-16}, 1.4 \times 10^{-14})$
DHF	p_2	$(9.4 \times 10^3, 2.9 \times 10^4)$
DHF	γ_2	$(-6.9 \times 10^{-12}, 4.9 \times 10^{-11})$
DHF	γ_E	$(1.4 \times 10^{-13}, 1.7 \times 10^{-13})$

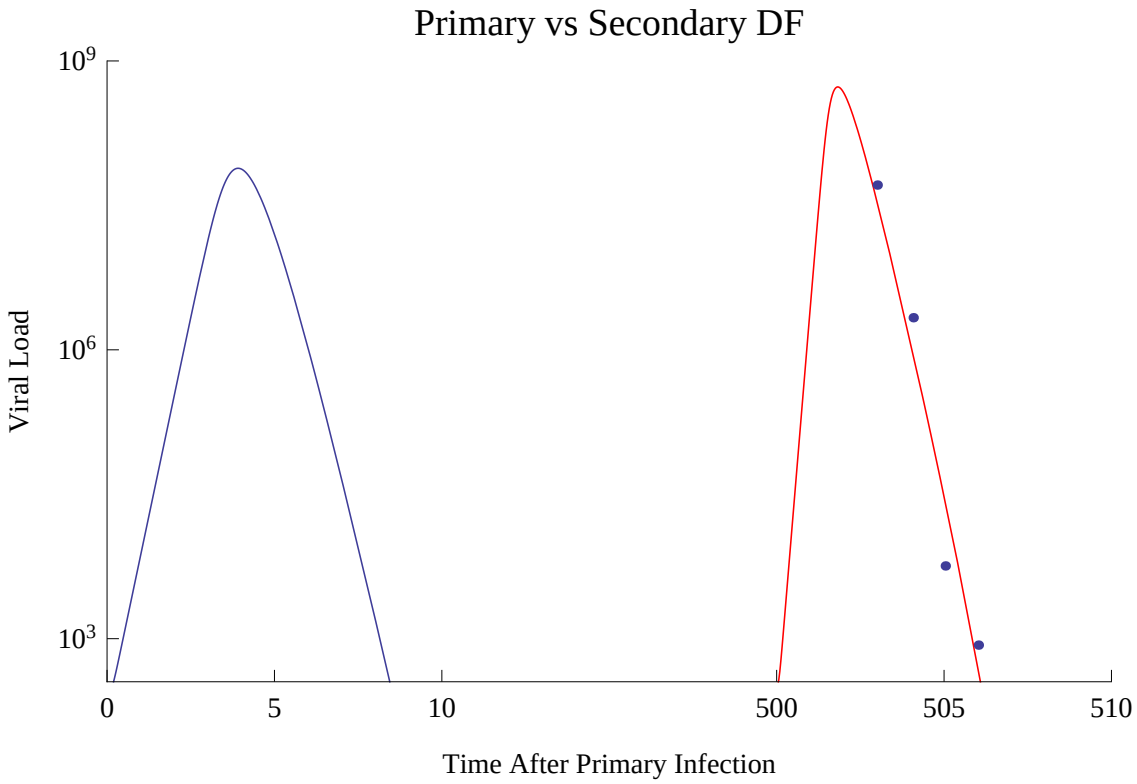

Figure 4.8: Viral load of secondary infection resulting in DF using parameters in Table 4.2a.

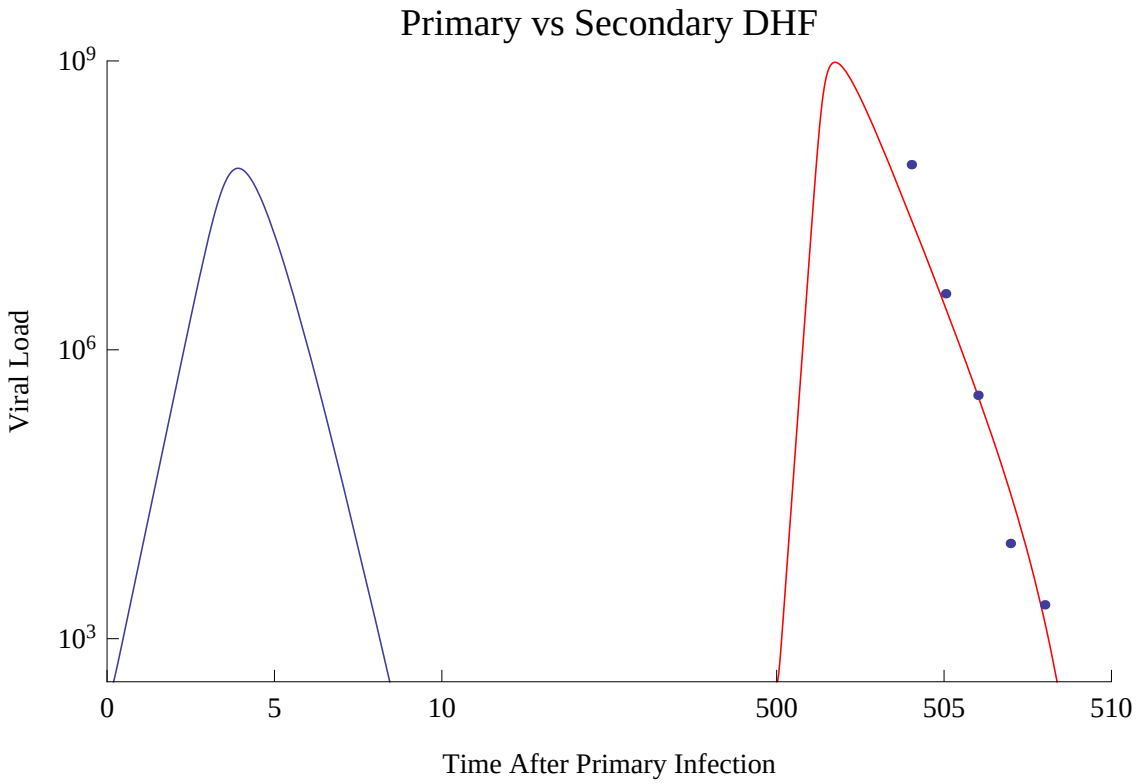

Figure 4.9: Viral load of secondary infection resulting in DHF using parameters in Table 4.2b.

We find that these results are more consistent with the known dynamics of DF and DHF because the viral peak of DHF is higher, the time of viral clearance of DHF is later, and the viral peak times are similar. We describe the specific results in the next section. Thus, the non-neutralizing antibodies clear the virus at a lower rate, leading to more severe infection. This may be explained by the fact that when the pre-existing antibody binds to the virus, phagocytes that would normally ingest this antibody-virus complex do not recognize it as something to be ingested since the antibody is not specific to the secondary virus. This leads to more virus being present in the body while not being cleared, thus leading to more severe infection.

Heterologous infections resulting in DF or DHF

Data fitting shows that during heterologous infections resulting in DF, the production rate of the second virus is three times higher than that of the first virus, *i.e.*, $p_2 = 3p_1 = 2 \times 10^4$ per infected cell per day. The strain-specific antibody-induced virus clearance is similar to that of the primary infection, *i.e.*, $\gamma_2 = 7 \times 10^{-10}$ ml per antibody per day, compared to

$\gamma_1 = 8 \times 10^{-10}$ ml per antibody per day. The decrease in virus clearance due to cross-reactive antibodies is small, $\gamma_E = 7.4 \times 10^{-15}$ ml per antibody per day. If we rewrite the clearance rate of the second virus to include the cross-reactive antibody-mediated decrease, *i.e.*,

$$c_2 = c - \gamma_E A_1 = c - \gamma_E K_A, \tag{4.40}$$

we obtain that $c_2 = 4.8$ per day, 4% smaller than the clearance rate of the first virus, $c = 5$ per day.

Data fitting shows that during heterologous infections resulting in DHF, the production rate of the second virus is $p_2 = 2 \times 10^4$ per infected cell per day, as in DF heterologous cases. The strain-specific antibody-induced virus clearance in DHF is $\gamma_2 = 2.1 \times 10^{-11}$ ml per antibody per day, 32-times smaller than the rate in DF heterologous cases $\gamma_2 = 7 \times 10^{-10}$ ml per antibody per day. The decrease in virus clearance due to cross-reactive antibody $\gamma_E = 1.6 \times 10^{-13}$ ml per antibody per day is 21-times higher than in the DF cases $\gamma_E = 7.4 \times 10^{-15}$ ml per antibody per day. If we rewrite the clearance rate of the second virus to include the cross-reactive antibody-mediated decrease, we obtain that $c_2 = 1.96$ per day, 2.45-times smaller than in the DF heterologous cases.

We compared the secondary DF and DHF cases for the estimated parameters (see red lines in Figs. 4.8 and 4.9). We find that the maximum virus concentration during secondary DHF cases is 1.8-times higher than that of secondary DF cases, *i.e.* 9.7×10^8 compared to 5.4×10^8 RNA per ml, as reported experimentally [37]. Viruses peak at similar times in both secondary DF and DHF cases, *i.e.*, 1.8 and 1.7 days following virus detection, as reported experimentally [36]. Lastly, viruses are cleared 6 and 8.4 days following virus detection, in secondary DF and DHF cases respectively, similar to experimental observations [39]. We summarize these results in Table 4.4.

Table 4.4: Comparison of Secondary DF and DHF Viral Dynamics

Disease Level	Viral Peak (RNA/ml)	Viral Peak Time (days)	Clearance Time (days)
DF	5.8×10^8	1.8	6.1
DHF	9.6×10^8	1.7	8.3

Primary versus secondary heterologous infections

We determined the differences between the dynamics of primary and secondary DF and DHF cases as given by models (4.1) and (4.29) and parameters in Tables 4.1 and 4.2 (see blue versus red lines in Figs. 4.8 and 4.9). We assume that the second virus is detected 500 days after the first virus detection. Thus the target cells have rebounded to the original number T_0. We also assume that the B-cells have rebounded to their original number B_0.

When both primary and secondary heterologous infections result in mild DF, the model predicts 7-times increase in the maximum viral concentration in secondary compared to primary

infections, *i.e.*, 5.4×10^8 virus per ml versus 7.7×10^7 virus per ml, as observed experimentally [37]. The viruses peak at 1.8 days and are cleared at day 6.1 during secondary DF infections compared to 3.9 days and 8.5 days during primary DF, as seen experimentally [36]. Lastly, the virus decay from the peak is faster during secondary DF infections, as reported experimentally [37] (see blue versus red lines in Fig. 4.8). These results are summarized in Table 4.5.

Table 4.5: Comparison of Primary DF and Secondary DF Viral Dynamics

Disease Level	Viral Peak (RNA/ml)	Viral Peak Time (days)	Clearance Time (days)
Primary	7.7×10^7	3.9	8.4
DF	5.8×10^8	1.8	6.1

When the secondary infections result in severe DHF, we predict an even higher maximum virus concentration, 9.7×10^8 virus per ml, 12-times higher than in the primary DF infections. Viruses reach their maximum 1.75 days after virus detection, as in the secondary DF infections. Interestingly, viruses are cleared at the same time as in the primary infection, 8.4 days virus detection, in contradiction to [37]. Lastly, viruses decay faster in DHF secondary cases compared to DF primary cases, similar to DF secondary cases (see blue versus red lines in Fig. 4.9). These results are summarized in Table 4.6.

Table 4.6: Comparison of Primary DF and Secondary DHF Viral Dynamics

Disease Level	Viral Peak (RNA/ml)	Viral Peak Time (days)	Clearance Time (days)
Primary	7.7×10^7	3.9	8.4
DHF	9.6×10^8	1.7	8.3

Initial Conditions

The estimates in our models are biased by our choice of initial conditions. In both primary and secondary infections, we started the models at the time of virus detection and the estimated parameters are sensitive to this choice. Indeed, in the primary infection model, a 10% reduction in the virus load requires 16% increase in the infectivity rate β for the quantitative behavior of model (4.1) to be preserved. Most importantly, when modeling secondary infections we assumed that the target monocytes and B cells reverted to their uninfected levels and the antibody to the first virus reached its maximum value, K_A, at the time of secondary infection. We modified this assumption such that $(T, I_1, V_1, B, B_{a1}, P_1, A_1)(\tau)$ is given by model (4.1) at the time τ when the second virus is detected. We showed that, for the parameters in Table 4.2a, secondary infections that occur close to primary infections have smaller magnitude (Fig 4.10) and delayed growth (Fig 4.11).

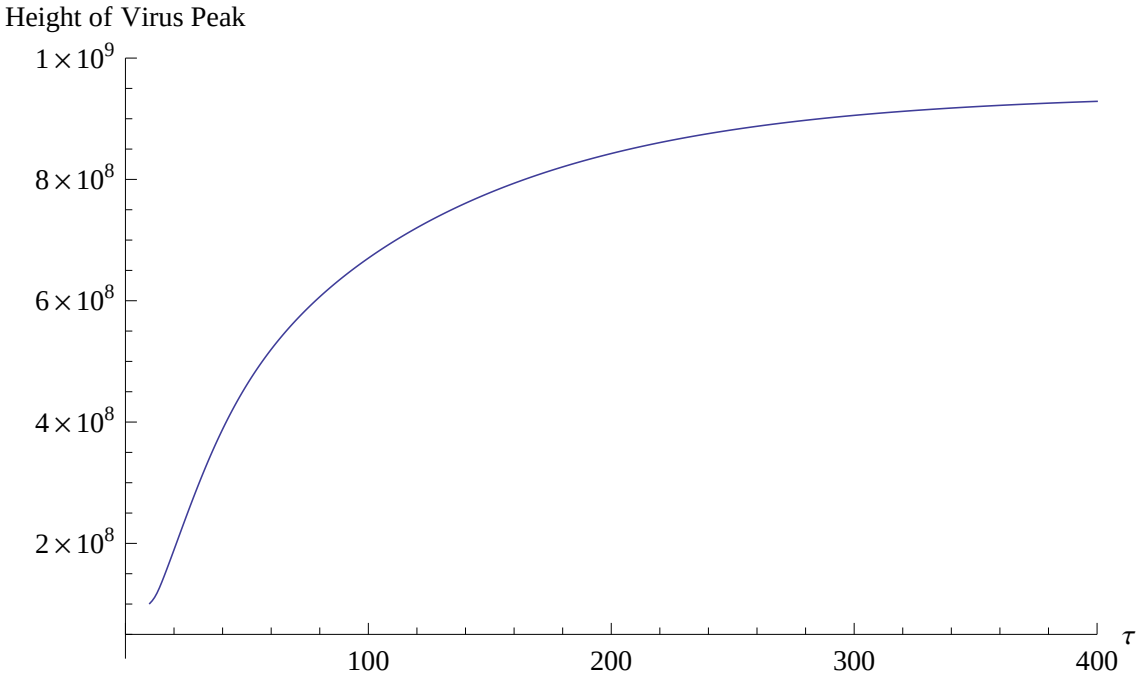

Figure 4.10: Change in height of virus peak depending on time when secondary virus enters.

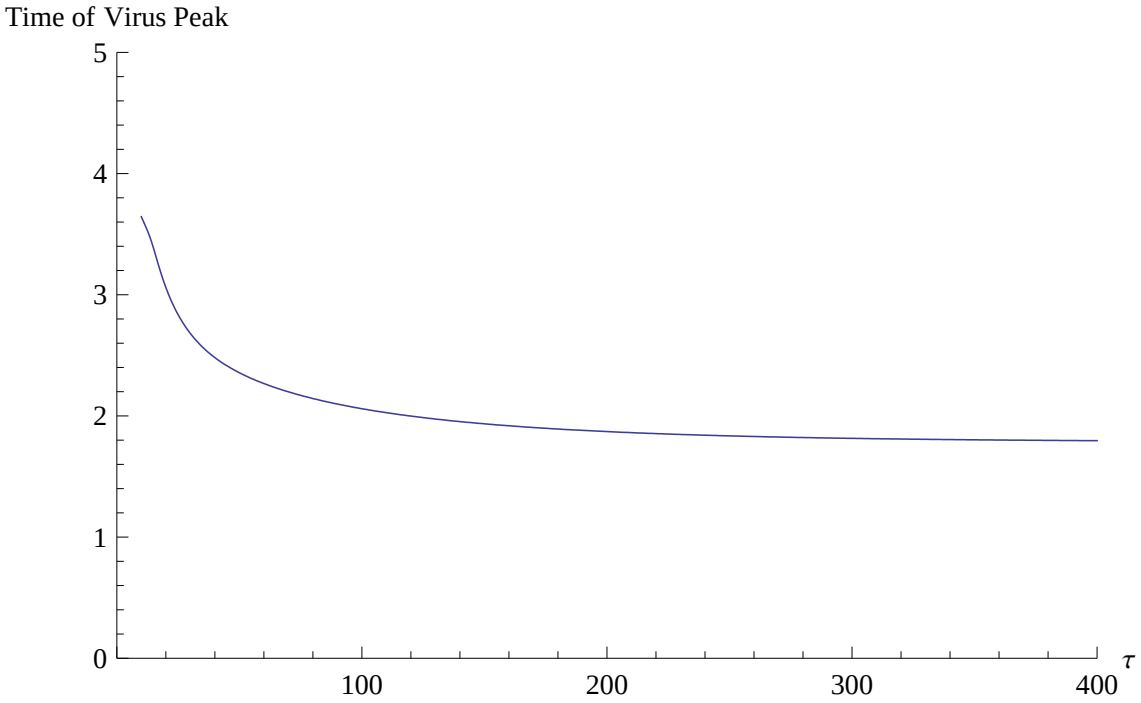

Figure 4.11: Change in time of virus peak depending on time when secondary virus enters.

This behavior is due to smaller concentration of target cells and fewer cross-reactive antibodies capable of interfering with viral clearance. We can also modify the initial number of antibodies specific to primary infection to determine how it affects the course of infection. Even though we assume antibodies stay at a steady state due to the time frame of our model, in reality, these antibodies decrease over long periods of time. Changing the initial number of antibodies will correlate with decreased severity of infection. These results can be used in a multi-scale model as described in Chapter 6.

4.3 Discussion

We developed a mathematical model of antibody responses to dengue primary infection and used it to determine unknown parameters that describe observed host-virus quantitative characteristics, such as high level viremia followed by virus clearance and delayed antibody responses which become detectable after virus resolution. We assumed that antibodies are present at levels below detection at the time of infection and modeled the neutralizing and non-neutralizing effects of antibody on virus evolution. We showed that both antibody functions are important for virus clearance, with the neutralizing rate having the strongest effect on viral reduction.

We expanded the model to secondary infections and determined the changes in virus and antibody during mild dengue fever and severe dengue hemorrhagic fever. We showed that secondary infections with the same serotype are cleared immediately, while secondary infections with a different serotype create higher viremia in both dengue fever and dengue hemorrhagic fever cases. The virus, however, is cleared faster during dengue fever-inducing secondary infections.

We used the model to determine the role of cross-reactive antibodies during secondary heterologous infections by fitting the models to published patient data [39]. Experimental studies have suggested that antibodies are responsible for increased infection of susceptible cells, as long-lived antibodies to the first virus bind the second virus without neutralizing it and, consequently, infect the phagocytes recruited to kill the immune complexes [14, 16, 30, 41]. Our model, however, cannot explain the biological data when it assumes enhancement of the infectivity rate of the second virus. Instead, data is explained when the presence of cross-reactive antibody results in the decrease of the overall heterologous virus clearance. One biological explanation for this result may be that, by binding to heterologous virus, cross-reactive antibodies render it unavailable for binding and subsequent removal by strain-specific antibodies through antibody-dependent cell-mediated viral inhibition (ADCVI) and/or antibody-dependent cell-mediated cytotoxicity (ADCC) [9]. Such non-neutralizing activity has been shown to occur during dengue infections [23], with unclear roles in protection [25] or pathogenesis [9].

Another explanation is that we are actually accounting for a reduction in the infected cells

removal rate, as the virus clearance rate c and infected cells death rate δ have similar effects on virus dynamics. Indeed, if we fit δ instead of γ and γ_E, we obtain a reduction in the infected cells killing rate during heterologous dengue hemorrhagic fever cases, but not in the heterologous dengue fever cases. This would imply that T cells specific for the first virus bind the heterologous virus leading to a reduction in their killing as suggested by the original antigenic sin phenomenon [17, 26, 28, 29]. Further work is needed to determine if a model of T cell cross-reactivity and original antigenic sin can explain the patient data. We discuss a possible model in chapter seven.

We have derived basic reproductive numbers corresponding to primary and secondary infections which show the relation between virus parameters, antibody parameters, and virus clearance. Since all dengue infections are acute regardless of the severity of the induced disease, our models assume that, following an initial viremia, the virus is cleared. Consequently, $R_0^p < 1$ and $R_0^s < 1$. However, we have showed that $R_0^p < R_0^s$ in both dengue fever and dengue hemorrhagic fever-induced secondary infections. This is due to increased virus production and decreased antibody-mediated protection.

In conclusion, we have developed and analyzed a within host model of dengue infections and derived parameters that may explain the virus dynamics during primary and secondary infections. We investigated the roles of strain-specific and cross-reactive antibodies in disease pathogenesis and predicted that the cross-reactive antibodies may account for disease enhancement leading to dengue hemorrhagic fever. Their role, however, is to decrease the clearance of the second virus, and therefore, interfere with the strain-specific non-neutralizing antibody activities. The results discussed in the chapter have been submitted to *Math Biosciences* [33].

Chapter 5

An Epidemiological Model of Dengue Viral Infection

5.1 Model Overview

We now want to describe an epidemiological model of dengue infection. Based on the model described in Chapter 3.3 [7], we can partition the overlapping compartments so that the model will be simpler to work with and relate more closely to the standard SIR model. Thus S represents the proportion of susceptible individuals, I_{ij} represents the proportion of individuals currently suffering a primary ($j = p$) or secondary ($j = s$) infection of strain $i = 1, 2$, R_i represents the proportion of individuals recovered from an infection caused by strain i (and thus susceptible to a secondary infection of the other strain), and R_{12} the proportion recovered from infections from both strains. We also have the transmission rate β_i for those with primary infection. Since secondary infection leads to more severe disease, it is assumed that the enhancement effect in secondary infection leads to transmission rate $\beta_i\phi_i$ for those with secondary infection where $\phi_i > 1$. Infections last for $1/\sigma$ years and birth and death rates are given by μ. Thus, the model is

$$
\begin{aligned}
\frac{dS}{dt} &= \mu - \beta_1 I_{1p} S - \beta_1 \phi_1 I_{1s} S - \beta_2 I_{2p} S - \beta_2 \phi_2 I_{2s} S - \mu S \\
\frac{dI_{1p}}{dt} &= \beta_1 I_{1p} S + \beta_1 \phi_1 I_{1s} S - \sigma I_{1p} \\
\frac{dI_{2p}}{dt} &= \beta_2 I_{2p} S + \beta_2 \phi_2 I_{2s} S - \sigma I_{2p} \\
\frac{dI_{1s}}{dt} &= \beta_1 I_{1p} R_2 + \beta_1 \phi_1 I_{1s} R_2 - \sigma I_{1s} \\
\frac{dI_{2s}}{dt} &= \beta_2 I_{2p} R_1 + \beta_2 \phi_2 I_{2s} R_1 - \sigma I_{2s} \\
\frac{dR_1}{dt} &= \sigma I_{1p} - \beta_2 I_{2p} R_1 - \beta_2 \phi_2 I_{2s} R_1 - \mu R_1 \\
\frac{dR_2}{dt} &= \sigma I_{2p} - \beta_1 I_{1p} R_2 - \beta_1 \phi_1 I_{1s} R_2 - \mu R_2 \\
\frac{dR_{12}}{dt} &= \sigma I_{1s} + \sigma I_{2s} - \mu R_{12}
\end{aligned}
\tag{5.1}
$$

Using this model, we can compare its solution with dengue epidemiological data and determine if enhancement affects the epidemiology of dengue.

5.2 Numerical Results

We first show the results from the model described in [7]. In the figure below, using the model from chapter 3.3, parameters $\mu = 1/50$, $\sigma = 100$, $\beta_1 = \beta_2 = 200$, and $\phi_1 = \phi_2 = 2.5$, and initial conditions $x_1 = .75$, $x_2 = .8$, $y_1 = 2.7 \times 10^{-5}$, $y_{21} = 1.4 \times 10^{-5}$, $y_2 = 1.1 \times 10^{-4}$, $y_{12} = 6.8 \times 10^{-5}$. Using the fact that z, the percentage of the population that has been infected with both strains, is $x_1 + x_2 - (1 - s)$, we let $z = .65$, and thus get the initial condition $s = .1$. We plot those infected with strain 1 x_1 (red), those infected with strain 2 x_2 (blue), and those infected with both strains $x_1 + x_2 - (1 - s)$ (green).

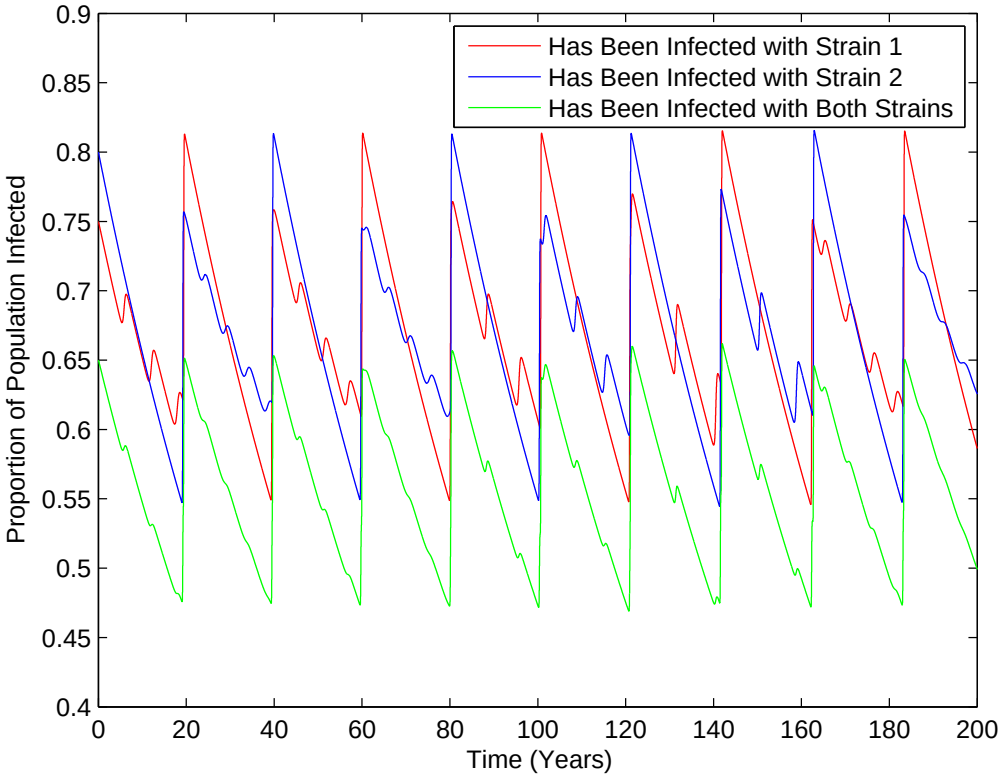

Figure 5.1: Results using the epidemiological model from Chapter 3.3.

The above is a predictive result due to what is known about the dynamics of dengue in a population. Over time, large fluctuations are seen in the number of cases of dengue infections as a result of different serotypes, even in the same population. These dynamics can be seen in Fig 5.2.

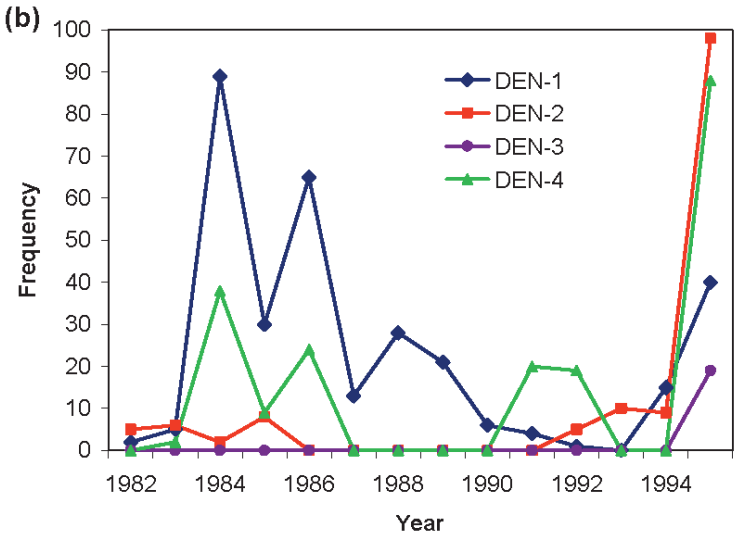

Figure 5.2: Number of dengue infections over time in a population in Mexico [7].

To show the similarities in the models, we plot those infected with strain 1 $R_{12}+R_1+I_{1p}+I_{1s}$ (red), those infected with strain 2 $R_{12}+R_2+I_{2p}+I_{2s}$ (blue), and those infected with both strains R_{12} (green) using the model described above. We use the same parameters as in the original model. However, the initial conditions are slightly different since we have split the overlapping compartments into separate compartments. So, we use initial conditions $S = .1$, $R_{12} = .65$, $R_1 = .0996$, $R_2 = .1498$, $I_{1p} = 2.7 \times 10^{-5}$, $I_{1s} = 1.4 \times 10^{-5}$, $I_{2p} = 1.1 \times 10^{-4}$, $I_{2s} = 6.8 \times 10^{-5}$ The results are shown in Fig 5.3.

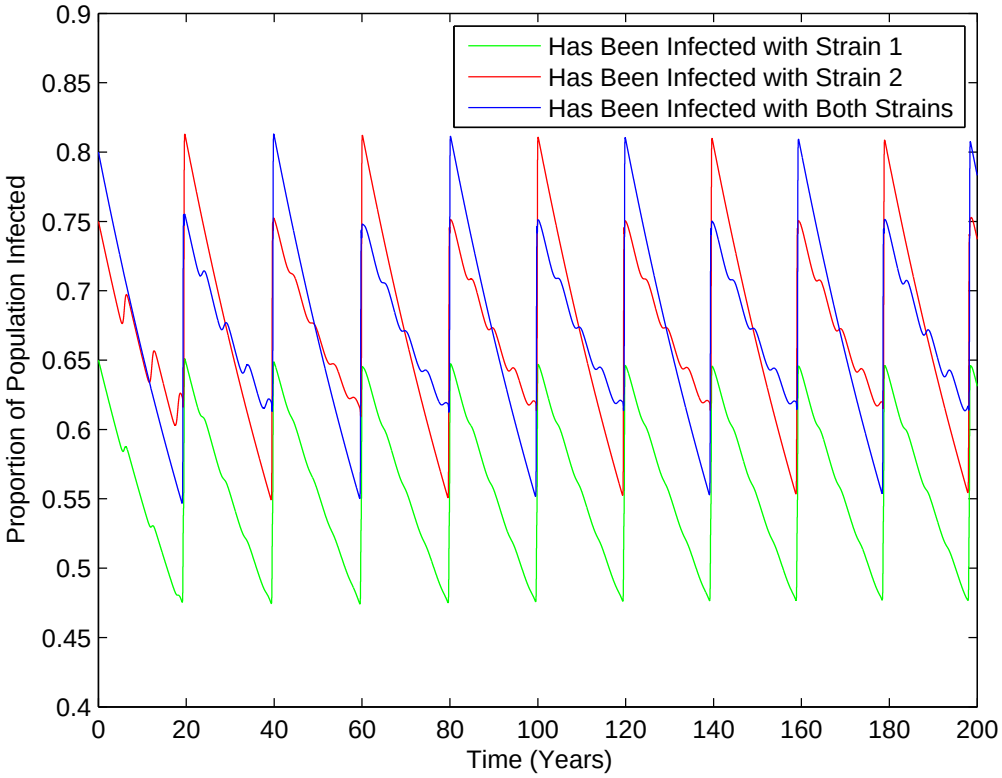

Figure 5.3: Results using the epidemiological model from Chapter 5.1.

We also can plot the infected population I_{1p} (red), I_{1s} (black), I_{2p} (green) and I_{2s} (blue) in Fig. 5.4.

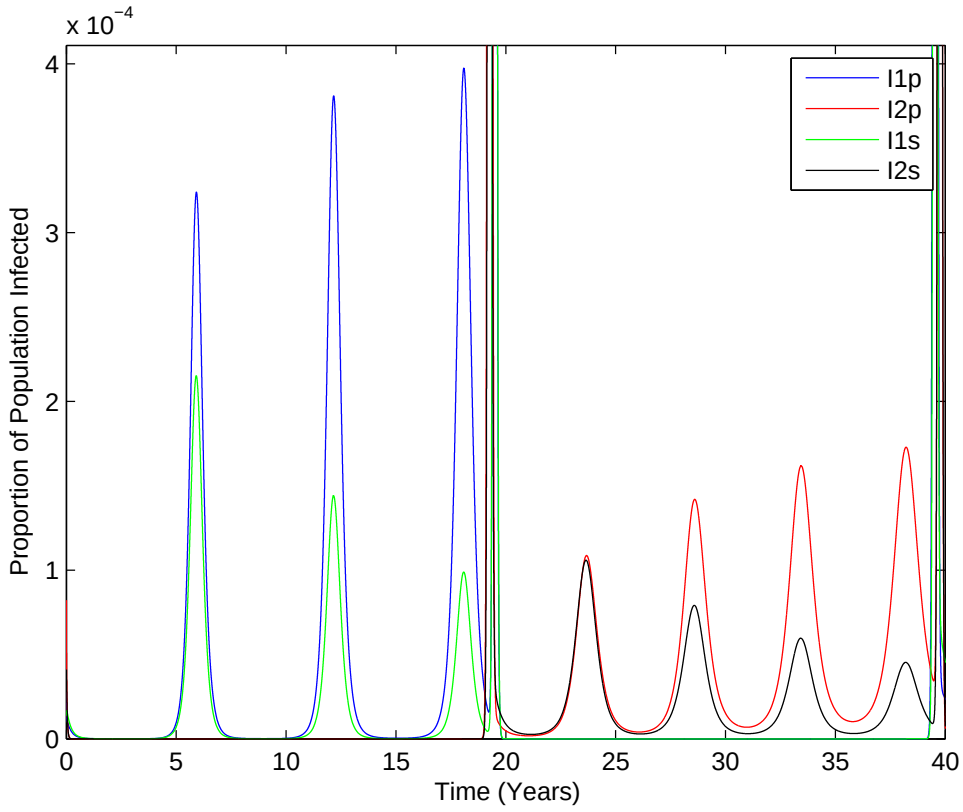

Figure 5.4: Infected population using the epidemiological model from Chapter 5.1.

The results from this model show that the infected population of each serotype fluctuates largely over time, which is consistent with the known epidemiology of dengue virus, as seen in Fig 5.2. In the case where there is no enhancement, *i. e.* $\phi_1 = \phi_2 = 1$, it can be shown that the solutions go to steady states. Therefore, we can conclude that the fluctuations in the epidemiology of dengue are dependent on the enhancement effect. We use this knowledge to develop a multi-scale model in the next chapter which incorporates the results from the within-host model and the epidemiological model.

Chapter 6

Multi-Scale Modeling

In chapter four, we discovered that the clearance rate by the non-neutralizing antibodies in primary infection is approximately twice that of secondary infection. Therefore, using the epidemiological model, instead of treating ϕ as a constant, we set $\phi = 1 + e^{-at}$. In contrast to the within-host model, the number of strain-specific antibodies actually decay over long periods of time, although they effectively stay at a steady state within the time frame we were observing in the within-host model. Therefore, initially, the transmission rate for secondary infections will be $2\beta_i$. However, over time, the strain-specific antibodies will decrease and thus the transmission rate will settle back on β_i, although an individual will die before it gets all the way back to β_i. So, using this model with the same initial conditions and parameters as described for the simulations of the model in Chapter 5.1 (except for phi_i), we find that for values of $a > 1.5$, the model ceases to have oscillations, and the compartments go to steady states. As an example, these dynamics are shown in Fig 6.1. This corresponds to the antibodies from the primary infection decaying relatively quickly, thus leading to secondary infection of a heterologous serotype acting similarly to primary infection. Thus, the transmission rates $\beta_i \approx \phi_i\beta_i$, implying $\phi_i \approx 1$. When using the model in Chapter 5.1 with constant rates $\phi_i = 1$, we observe that oscillations cease to occur as well. So, this particular multi-scale model gives results that are similar to the dynamics of the epidemiological model alone. In the next chapter, we discuss a different multi-scale model that may yield different results than the epidemiological model.

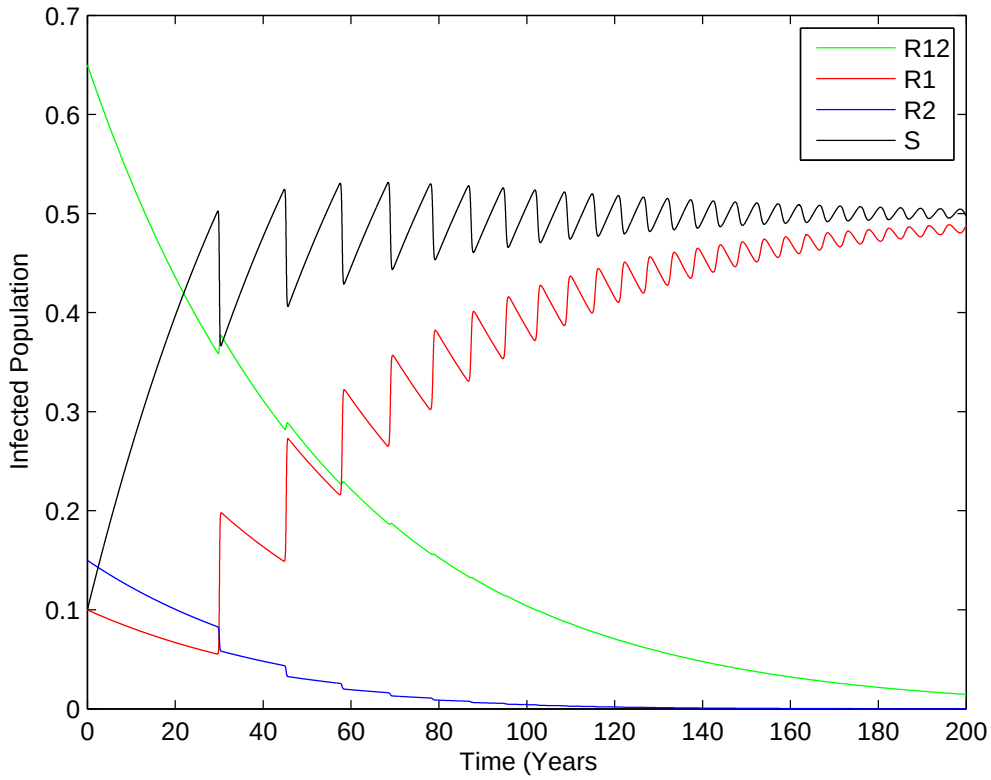

Figure 6.1: Results using the multi-scale model from chapter 6 for $a = 1.6$.

Chapter 7

Future Work

Based on the results from our within-host model, we determined that viral clearance is reduced in secondary infection. However, we mentioned that another explanation for this result may be that we are accounting for a reduced rate of the removal of infected cells due to original antigenic sin, which has been explained previously in chapter two. We plan to develop a model to describe original antigenic sin and see how well it fits with the dengue patient data. We describe an original antigenic sin model using terms and parameters similar to those the ADE model, ignoring the effect from antibodies. We include strain-specific CD8 T-cells (effector cells) E, which interact with infected cells at rate ϕ and cause more effector cells to be produced. We assume that effector cells clear the infected cells at rate μ. However, when effector cells from the primary infection interact with infected cells from the secondary infection, they clear the infected cells at rate μ_2, which may possibly be negative due to original antigenic sin. Thus, the model is

$$\begin{aligned}
\frac{dT}{dt} &= s - d_T T - \beta_1 T V_1 - \beta_2 T V_2, \\
\frac{dE_i}{dt} &= s_E + \phi E_i I_i - d_E E_i, \\
\frac{dI_1}{dt} &= \beta_1 T V_1 - \mu E_1 I_1 - \delta I_1, \\
\frac{dI_2}{dt} &= \beta_2 T V_2 - (\mu E_2 I_2 + \mu_2 E_1 I_2) - \delta I_1, \\
\frac{dV_1}{dt} &= p_1 I_1 - (c + \gamma_1 A_1) V_1, \\
\frac{dV_2}{dt} &= p_2 I_2 - c V_2.
\end{aligned} \tag{7.1}$$

We also plan to develop an epidemiological model that takes into account vaccination and vector terms, similar to the models described in chapter three. We plan to expand on the idea of multi-scale modeling of dengue, using a more complex epidemiological model which

incorporates the results from our within-host model.

We describe a possible model similar to the one described in Chapter 6, but which does not assume exponential decay of antibodies. Instead, we base our model on the one described by Heffernan in Chapter 3.4. We assume that the more strain-specific antibodies present from primary infection, the stronger the ADE effect will be. Since the clearance rate in DHF is approximately 2.5 times smaller than that of primary infection (as found in the within-host model), this corresponds to $\phi_1 = \phi_2 = 2.5$. Using the within-host model, we can calculate other ϕ for different starting levels of antibodies from primary infection, which will be lower than 2.5. We can assume that the antibodies decrease to a different level at a fixed time $\frac{1}{\alpha}$. Using i levels, the new model is

$$\begin{aligned}
\frac{dS}{dt} &= \mu - \beta_1 I_{1p} S - \sum_i (\beta_1 \phi_{1_i} I_{1s_i} S) - \beta_2 I_{2p} S - \sum_i (\beta_2 \phi_{2_i} I_{2s_i} S) - \mu S \\
\frac{dI_{1p}}{dt} &= \beta_1 I_{1p} S + \sum_i (\beta_1 \phi_{1_i} I_{1s_i} S) - \sigma I_{1p} \\
\frac{dI_{2p}}{dt} &= \beta_2 I_{2p} S + \sum_i (\beta_2 \phi_{2_i} I_{2s_i} S) - \sigma I_{2p} \\
\frac{dI_{1s_i}}{dt} &= \beta_1 I_{1p} R_{2_i} + \sum_j \left(\beta_1 \phi_{1_j} I_{1s_j} R_{2_i}\right) - \sigma I_{1s_i} \\
\frac{dI_{2s_i}}{dt} &= \beta_2 I_{2p} R_{1_i} + \sum_j \left(\beta_2 \phi_{2_j} I_{2s_j} R_{1_i}\right) - \sigma I_{2s_j} \\
\frac{dR_{1_i}}{dt} &= \sigma I_{1p} + \alpha R_{1_{i+1}} - \beta_2 I_{2p} R_{1_i} - \sum_j \left(\beta_2 \phi_{2_j} I_{2s_j} R_{1_i}\right) - \alpha R_{1_i} - \mu R_{1_i} \\
\frac{dR_{2_i}}{dt} &= \sigma I_{2p} + \alpha R_{2_{i+1}} - \beta_1 I_{1p} R_{2_i} - \sum_j \left(\beta_1 \phi_{1_j} I_{1s_j} R_{2_i}\right) - \alpha R_{2_i} - \mu R_{2_i} \\
\frac{dR_{12}}{dt} &= \sum_i \sigma I_{1s_i} + \sum_i \sigma I_{2s_i} - \mu R_{12}
\end{aligned} \tag{7.2}$$

We plan to work with this model to determine if it gives us different dynamics that can not be found using constant rates for parameters in the original model as described in Chapter 5.1.

Based on the results from our future work, we hope to have a more complete set of models that can consistently describe the behavior of dengue viral infection within hosts and within a population. The ultimate goal of this research is to determine how best the spread of dengue virus can be controlled and whether vaccination will lead to undesirable consequences in populations. To gain a better understanding of how dengue virus permeates through a population, we must take into account the virus-host interaction, the period of cross-protection, and the effect of enhancement when estimating the rate of transmission between

hosts. We also must consider transmission rates from human to mosquito populations. While there is currently a dengue vaccination trial being conducted, the effects of vaccination are unknown. Mathematical modeling derived from an understanding of the pathology of dengue virus is the best tool we have to predict these unknown long-range outcomes.

Bibliography

[1] B. Alberts, A. Johnson, J. Lewis, M. Raff, K. Roberts, and P. Walter. *Molecular Biology of the Cell*. Garland Science, New York, 4 edition, 2002.

[2] S. Alcon, A. Talarmin, M. Debruyne, A. Falconar, V. Deubel, and M. Flamand. Enzyme-linked immunosorbent assay specific to dengue virus type 1 nonstructural protein NS1 reveals circulation of the antigen in the blood during the acute phase of disease in patients experiencing primary or secondary infections. *J Clin Microbiol*, 40:376–381, 2002.

[3] C. Beauchemin and A. Handel. A review of mathematical models of influenza A infections within a host or cell culture: lessons learned and challenges ahead. *BMC Public Health*, 11:S1–S15, 2011.

[4] D. Bortz and P. Nelson. Sensitivity analysis of a nonlinear lumped parameter model of HIV infection dynamics. *Bull Math Biol*, 66:1009–1026, 2004.

[5] H. Dahari, R. Ribeiro, and A. Perelson. Mathematical models of HIV pathogenesis and treatment. *Bioessays*, 24:1178–87, 2002.

[6] R. Duffin and R. Tullis. Mathematical models of the complete course of HIV infection and AIDS. *J Theor Med*, 4:215–221, 2002.

[7] N. Ferguson, R. Anderson, and S. Gupta. The effect of antibody-dependent enhancement on the transmission dynamics and persistence of multiple-strain pathogens. *Proc Natl Acad Sci USA*, 96:790–794, 1999.

[8] S. Fry, M. Meyer, M. Semple, C. Simmons, S. Sekaran, J. Huang, C. McElnea, C.-Y. Huang, A. Valks, P. Young, and M. Cooper. The diagnostic sensitivity of dengue rapid test assays is significantly enhanced by using a combined antigen and antibody testing approach. *PLoS Negl Trop Dis*, 5:e1199, 2011.

[9] G. Garcia, M. Arango, A. Prez, L. Fonte, B. Sierra, R. Rodrguez-Roche, E. Aguirre, I. Fiterre, and M. Guzman. Antibodies from patients with dengue viral infection mediate cellular cytotoxicity. *J Clin Virol*, 37:53–57, 2006.

[10] S. Goldstein, F. Zhou, S. Hadler, B. Bell, E. Mast, and H. Margolis. A mathematical model to estimate global hepatitis B disease burden and vaccination impact. *Int J Epidemiol*, 34:1329–1339, 2005.

[11] D. Gubler. Dengue and dengue hemmoragic fever. *Clin Microbiol Rev*, 11:480–493, 1998.

[12] M. Guzman, M. Alvarez, R. Rodriguez-Roche, L. Bernardo, T. Montes, S. Vazquez, L. Morier, A. Alvarez, E. Gould, G. Kour, and S. Halstead. Neutralizing antibodies after infection with dengue 1 virus. *Emerg Infect Diseases*, 13:283–286, 2007.

[13] M. Guzman, M. Alvarez, and H. S. Secondary infection as a risk factor for dengue hemorrhagic fever/ dengue shock syndrome: an historical perspective and role of antibody-dependent enhancement of infection. *Arch Virol*, 158:1445–1459, 2013.

[14] M. Guzman, G. Kouri, L. Valdes, J. Bravo, S. Vazquez, and S. Halstead. Enhanced severity of secondary dengue-2 infections: death rates in 1981 and 1997 Cuban outbreaks. *Rev Panam Salud Publica*, 11:223–227, 2002.

[15] S. Halstead. Dengue. *Lancet*, 370:1644–52, 2007.

[16] S. Halstead, S. Mahalingam, M. Marovich, S. Ubol, and D. Mosser. Intrinsic antibody-dependent enhancement of microbial infection in macrophages: Disease regulation by immune complexes. *Lancet Infect Dis*, 10:712 – 722, 2010.

[17] S. Halstead, S. Rojanasuphot, and S. N. Original antigenic sin in dengue. *Am J Trop Med Hyg*, 32:154–156, 1983.

[18] A. Handel, J. Brown, D. Stallknecht, and P. Rohani. A multi-scale analysis of influenza A virus fitness trade-offs due to temperature-dependent virus persistence. *PLOS Computational Biology*, 9:e1002989, 2013.

[19] J. Heffernan and M. Keeling. Implications of vaccination and waning immunity. *Proc R Soc B*, 276:2071–2080, 2009.

[20] D. Ho, A. Neumann, A. Perelson, W. Chen, J. Leonard, and M. Markowitz. Rapid turnover of plasma virions and CD4 lymphocytes in HIV-1 infection. *Nature*, 373:123–126, 1995.

[21] W. Kermack and A. McKendrick. A contribution to the mathematical theory of epidemics. *Proc R Soc Lond*, 115:700–721, 1927.

[22] Z. Kou, J. Lim, M. Beltramello, M. Quinn, H. Chen, S. Liu, L. Martnez-Sobrido, M. Diamond, J. Schlesinger, A. de Silva, F. Sallusto, and X. Jin. Human antibodies against dengue enhance dengue viral infectivity without suppressing type I interferon secretion in primary human monocytes. *Virology*, 410:240–247, 2011.

[23] I. Kurane and F. Ennis. *Immunopathogenesis of dengue virus infections*, volume Dengue and Dengue Hemorrhagic fever. CAB International, Oxon, UK, 1997.

[24] J. Lang. Recent progress on sanofi pasteur's dengue vaccine candidate. *J Clin Virol*, 46:20–24, 2009.

[25] K. Laoprasopwattana, D. Libraty, T. Endy, A. Nisalak, S. Chunsuttiwat, F. Ennis, A. Rothman, and S. Green. Antibody-dependent cellular cytotoxity mediated by plasma obtained before secondary dengue virus infections: Potential involvement in early control of viral replication. *J Infect Dis*, 195:1108–1116, 2007.

[26] G. Malavigea and G. Oggb. T cell responses in dengue viral infections. *J Clin Virol*, 58:605 611, 2013.

[27] G. Marchuk, R. Petrov, A. Romanyukha, and G. Bocharov. Mathematical model of antiviral immune response I. data analysis, generalized picture construction and parameters evaluation for hepatitis B. *J Theor Biol*, 151:1–40, 1991.

[28] A. Mathew, I. Kurane, A. Rothman, L. Zeng, M. Brinton, and F. Ennis. Dominant recognition by human CD8+ cytotoxic T lymphocytes of dengue virus nonstructural proteins NS3 and NS1.2a. *J Clin Invest*, 98:1684 – 1692, 1996.

[29] J. Mongkolsapaya. Original antigenic sin and apoptosis in the pathogenesis of dengue hemorrhagic fever. *Nat Med*, 9:921–927, 2003.

[30] D. Morens. Antibody-dependent enhancement of infection and the pathogenesis of viral disease. *Clin Infect Dis*, 19:500–512, 1994.

[31] J. Mosquera, J. Hernandez, N. Valero, L. Espina, and G. Anez. Ultrastructural studies on dengue virus type 2 infection of cultured human monocytes. *J Virol*, 2:26, 2005.

[32] A. Neumann, N. Lam, H. Dahari, D. Gretch, T. Wiley, T. Layden, and A. Perelson. Hepatitis C viral dynamics in vivo and the antiviral efficacy of interferon- therapy. *Science*, 282:103–107, 1998.

[33] R. Nikin-Beers and S. Ciupe. The role of antibody in dengue viral infection. *Math Biosciences*, 2014. Submitted.

[34] N. Nuraini, H. Tasman, E. Soewono, and K. Sidarto. A with-in host dengue infection model with immune response. *Mathematical and Computer Modeling*, 49:1148–1155, 2009.

[35] M. Oprea and A. Perelson. Exploring the mechanism of primary antibody responses to T-cell-dependent antigen. *J Theor Biol*, 181:215–236, 1996.

[36] V. Tricou, N. Minh, J. Farrar, H. Tran, and C. Simmons. Kinetics of viremia and NS1 antigenemia are shaped by immune status and virus serotype in adults with dengue. *PLoS Negl Trop Dis*, 5:e1309, 2011.

[37] D. Vaughn, S. Green, S. Kalayanarooj, B. Innis, S. Nimmannitya, S. Suntayakorn, T. Endy, B. Raengsakulrach, A. Rothman, F. Ennis, and A. Nisalak. Dengue viremia titer, antibody response pattern, and virus serotype correlate with disease severity. *J Infect Dis*, 181, 2000.

[38] D. Vaughn, S. Green, S. Kalayanarooj, B. Innis, S. Nimmannitya, S. Suntayakorn, A. Rothman, F. Ennis, and A. Nisalak. Dengue in the early febrile phase:viremia and antibody responses. *J Infect Dis*, 176:322–330, 1997.

[39] W. Wang, H. Chen, C. Yang, S. Hsieh, C. Juan, S. Chang, C. Yu, L. Lin, J. Huang, and C. King. Slower rates of clearance of viral load and virus-containing immune complexes in patients with dengue hemorrhagic fever. *Clin Infect Dis*, 43:1023–1030, 2006.

[40] H. Wearing and P. Rohani. Ecological and immunologcial determinants of dengue epidemics. *Proc Natl Acad Sci*, 103:11802–11807, 2006.

[41] S. Whitehead, J. Blaney, A. Durbin, and B. Murphy. Prospects for a dengue virus vaccine. *Nature Reviews Microbiology*, 5:518–528, 2007.

[42] D. Wodarz and M. Nowak. *Hepatology*, 46:16–21, 2007.

[43] World Health Organization Dengue Vaccine Modeling Group. Assessing the potential of a candidate dengue vaccine with mathematical modeling. *PLoS Negl Trop Dis*, 6:e1450, 2012.

[44] J. Zalevsky, A. Chamberlain, H. Horton, S. Karki, I. Leung, T. Sproule, G. Lazar, D. Roopenian, and J. Desjarlais. Enhanced antibody half-life improves in vivo activity. *Nat Biotechnol*, 28:157–159, 2010.